Paper:

Riva, S., Yusenko, K., Lavery, N., Jarvis, D. & Brown, S. (2016). The scandium effect in multicomponent alloys.
International Materials Reviews, 61(3), 203-228.
http://dx.doi.org/10.1080/09506608.2015.1137692

_____

The Scandium Effect in Multicomponent Alloys

Sephira Riva*[1], Kirill V. Yusenko[1], Nicholas P. Lavery[1], David J. Jarvis[2], Stephen G.R. Brown**[1]

1 College of Engineering, Swansea University, Bay Campus, SA1 8QQ, Swansea, UK

2 European Space Agency, ESTEC, Keplerlaan 1, Noordwijk, NL

* 839245@swansea.ac.uk

** S.G.R.Brown@swansea.ac.uk

Abstract

Despite its excellent elemental properties, lightweight nature and good alloying potential, scandium has received relatively little attention in the manufacturing community. The abundance of scandium in the Earth's crust is quite high. It is more abundant than silver, cobalt, lead and tin. But, because scandium is so well dispersed in the lithosphere, it is notoriously difficult to extract in commercial quantities - hence low market availability and high cost. Scandium metallurgy is still a largely unexplored field - but progress is being made. This review aims to summarise advances in scandium metallurgical research over the last decade. The use of scandium as a conventional minor addition to alloys, largely in structural applications, is described. Also, more futuristic functional applications are discussed where details of crystal structures and peculiar symmetries are often of major importance. This review also includes data obtained from more obscure sources (especially Russian publications) which are much less accessible to the wider community. It is clear that more fundamental research is required to elevate the status of scandium from a laboratory-based curiosity to a mainstream alloying element. This is largely uncharted territory. There is much to be discovered.

Keywords Scandium, Alloys, Intermetallics, Phase diagrams, Mechanical properties

1. Introduction

Since the first days of powered flight, aircraft designers have focused on achieving minimum weight, both in airframes and in propulsion systems. Historically, the selection of materials was driven mostly by strength/weight ratio considerations. However, current design criteria have strict requirements for processing methods, safety and material specifics. Aluminium-lithium alloys, for example, were developed in Russia in the early 1960's (the so-called 1420 alloys). These alloys required heat treatment in order to increase their hardness and mechanical properties, but their composition, combined with new welding technology, allowed a decrease in aircraft mass of up to 20 %. Aluminium-beryllium alloys were also proposed to provide affordable alternatives to resin matrix composites in critical airframe components.[1]

In both cases, the danger involved in applying such reactive materials limited their active use. However, the introduction of Sc into the 1420 alloy, leading to an increase in yield strength of 20 – 25 % while decreasing rocket bodies mass by 10-15%, opened the doors for wider application of scandium in the aerospace industry.

Constructional parts of the giant airplane "*AN-124*" were produced from a modified variant of the Sc-containing 1420 alloy, the so-called 1421 alloy (according to the Russian classification).

Al – Cu – Li highly corrosion resistant alloys with zirconium and scandium additions were employed for cryogenic fuel tanks for spacecraft and aircraft. Tests proved their applicability for fuel tank applications, which decreased rocket mass by 35 %.[2]

The last ten years have brought about a renewed interest in scandium as a key element for the development of lighter materials for aerospace applications. A recent NASA report describes the use of Al─Sc-based alloys for fuel tanks and air frames, applications in which low weight and chemical stability to hydrogen peroxide are critical. Moreover, the recent ESA Grand Challenge, identified by FTAP in 2012, states that lightweight, stable, high-stiffness structures are a top priority for the Agency.[3]

As such, high performance scandium alloys could find numerous applications in primary satellite structures, cryogenic tanks, solar panel substrates, rocket nozzles and thrusters, re-entry hot structures, Mars rovers, electronic packaging and optical benches, as well as in armour development.[4]

The last detailed evaluation of Al-based scandium alloys and compounds was published over 10 years ago: the numerous papers published since then have mostly confirmed known results. Conversely, the purpose of this review is to collect and critically analyse recent

experimental data concerning scandium-based alloys and intermetallics, as well as rarely accessed data in PhD theses and journals.

1.1 Scandium properties

Scandium was first discovered in 1879 by Lars F. Nilson in Uppsala, Sweden. However, its limited availability and the intrinsic difficulties with its extraction delayed its study until fifty years later. It was only in 1937 that the first pound of pure elemental scandium metal was produced (Fisher *et alia*) by performing an electrolysis of molten scandium, lithium and potassium chlorides in a graphite crucible with a tungsten wire, using molten zinc as the working electrode. The first data on the investigation of scandium systems with other metals and on the synthesis of scandium compounds were published in the early sixties. Scandium is the first *d*-element, as well as being a member of the family of rare earths. Its peculiar features link it to the lanthanides and yttrium. In particular, scandium is a light metal with a density comparable with aluminium (2.989 gcm^{-3}) and a high melting temperature of 1814 K (close to the melting point of iron).

1.2 . Elemental scandium under high-temperature and high-pressure

Elemental scandium has been studied under high-temperature and very high-pressure. Under ambient pressure Sc has two forms: the low-temperature (α) *hcp* form, stable below 1337 °C, transforms into a high-temperature (β) *bcc* structure with a melting temperature of 1541 °C. Transition between alpha and beta phases have been investigated *in situ* using time-of-flight neutron diffraction (figure 1.2.1).[5]
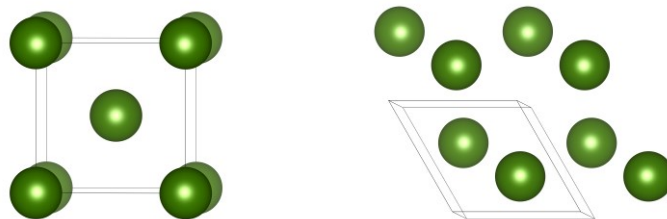
Figure 1.2.1. Crystal structure of room temperature *hcp* α (Sc) along *c*-axis (*left*) and high-temperature *bcc* β (Sc) (*right*).[5]
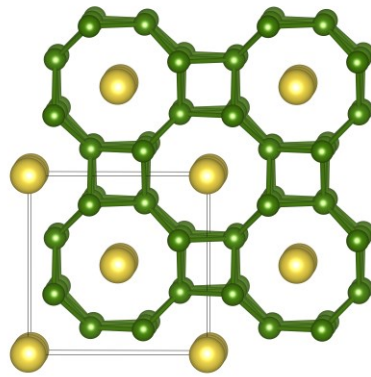
Figure 1.2.2. Crystal structure of high-pressure tetragonal incommensurate Sc-II phase along *c*-axis. The figure shows two crystallographically independent Sc atoms forming host framework (*yellow*) and guest atoms (*green*).[5]
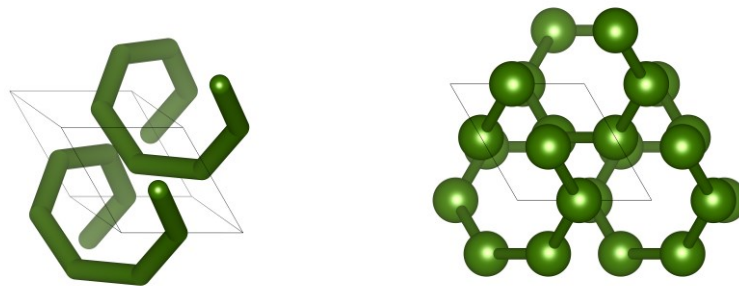
Figure 1.2.3. Crystal structure of high-pressure hexagonal Sc-V phase along *a*-axis (*left*) and *c*-axis (*right*).[5]

The high-pressure behaviour of elemental scandium has been intensively investigated during the last two decades using diffraction and magnetometry in diamond anvil cells up to 297 and 74 GPa respectively.[6] Under compression Sc shows five high-pressure modifications. None of these can be recovered after decompression. Schematically, high-pressure properties of Sc can be summarised as follows:

$$\frac{hcp - Sc - I}{ambient\ phase} \xrightarrow{17\ GPa} \frac{Sc - II}{I'\frac{4}{mcm}(0\ 0\ \gamma)} \xrightarrow{104\ GPa} Sc - III \xrightarrow{140\ GPa} Sc - IV$$

$$\xrightarrow{239\ GPa} \frac{Sc - V}{P6_122\ or\ P6_522}$$
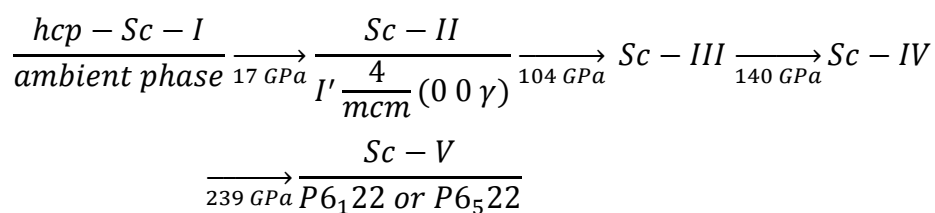
The crystal structures of Sc-II and Sc-V have been solved and refined using high-pressure powder X-ray diffraction. Both structures are quite complex (figures 1.2.2. and 1.2.3.). The crystal structure characteristic for Sc-II can only be described using incommensurate crystallography. In the structure, tetragonal host channels along the c-axis include incommensurate guest chains within the host lattice. The structural parameters for the host lattice were refined as $a_1=7.550$, $c_1=3.439$ and those for the guest lattice as $a_2 = a_1$, $c_2 = 2.281$ Å. The crystal structure can be solved in I' $4/mmc$ (00γ) four dimensional space group with the incommensurability γ, defined by c_1/c_2: its corresponding value has been refined as 1.508. The hexagonal Sc-V crystal structure can be derived from modulations of the inter-plane stacking of the (111) planes in an *fcc* arrangement. Both crystal structures are unique among all elements investigated under high-pressure. The crystal structures of phases Sc-III and Sc-IV seem to be quite complex and can probably be solved in low symmetry space groups, since diffraction patterns show many diffraction lines. These crystal structures are still unknown.

Ambient phase Sc-I does not show a superconducting transition. In contrast, Sc-II shows a superconducting transition below 5 K at 50 GPa. Critical temperature increases with pressure and reaches 19.7 K at 107 GPa. 19.7 K is the second highest superconducting temperature observed for pure elements investigated under pressure. The value reported is slightly lower in comparison with the maximum temperature of 25 K obtained for Ca compressed up to 161 GPa. The critical temperature observed for the Sc-II phase drops sharply to 8 K at the Sc-II → Sc-III boundary (107 GPa) and then rises slightly when pressure is increased. Electronic properties, as well as the nature of the superconducting state in Sc-II, have been theoretically investigated. In particular, recent studies highlighted the important role played by *d*-electrons in phase transitions under pressure.[7]

1.3 Extraction costs and natural occurrence

According to data published by the Scandium International Mining Corporation in 2015, scandium occurrence in minerals is around 22 ppm, making it more abundant than lead, mercury and precious metals. However, like other rare-earth elements, scandium rarely concentrates in nature over 100 ppm. As a consequence, no dedicated single mine source exists, and only 15 tonnes of scandium are produced globally each year. The only known concentrated sources of this elements are the following eight rare minerals: thortveitite

$[(Sc,Y)_2Si_2O_7]$ (which can contain up to 45% of scandium in its oxide form), bazzite $[Be_3(Sc, Al)_2Si_6O_{18}]$, cascandite $[Ca(Sc,Fe^{2+})-Si_3O_8(OH)]$, jervisite $[(Na,Ca,Fe^{2+})(Sc,Mg,Fe^{2+})Si_2O_6]$, kolbeckite $[ScPO_4*2H_2O]$, pretulite $[ScPO_4]$, juonnite $[CaMgSc(PO_4)_2OH*4H_2O]$ and kristiansenite, $[Ca_2ScSn(Si_2O_7)(Si_2O_6OH)]$.[8]

Thus scandium occurs in many ores but never in quantities sufficient for them to be considered deposits. As a consequence the metal is recovered as a by-product during the processing of residues of uranium leach liquors, titanium pigment production waste liquors, tungsten refining, *etc*.

Conventional methods to separate and concentrate scandium include metallurgical processes, precipitation/co-precipitation and solvent extraction. Among these only hydrometallurgical techniques (ore penetrating, leaching, solvent extraction, precipitation, calcination) lead to high-purity products with adequate selectivity and efficiency. However, this technology is sensitive to the interference of impurities associated with scandium extraction (especially during co-dissolution and co-extraction processes) and requires high acid consumption for the processing of low precious material quantities (during leaching with medium to concentrated mineral acids).[9]

Considering these extraction difficulties and process costs it is not surprising that, out of a global trade volume of less than 10 tons, only 400 kg comes from scandium primary production, while the rest originates from Russian stockpiles created during the Cold War. Since the deposits of Madagascar and Norway (rich in thortveitite and kolbeckite) are not exploited, in 2014 only three mines actively produced scandium: the uranium and iron mines in Zhovti Vody, Ukraine; the rare earth mines in Bayan Obo, China; the apatite mines in the Kola peninsula, Russia.

A consistent supply may bring forth wider applications for scandium, whose latent demand, according to research from Kaiser, is expected to reach over 300 tons by 2025. Currently, no corporation can produce enough scandium to meet this target. However, Platina Resources, Metallica Minerals Ltd and EMC Metals Corporation (in a joint venture with Jervois Mining Ltd.) are currently moving towards the exploitation of Australian ores and expect to be able to supply 9100 tons, 50-65 tons and 25 tons respectively of 99.9% pure scandium by 2017.

1.4 Scandium in industry
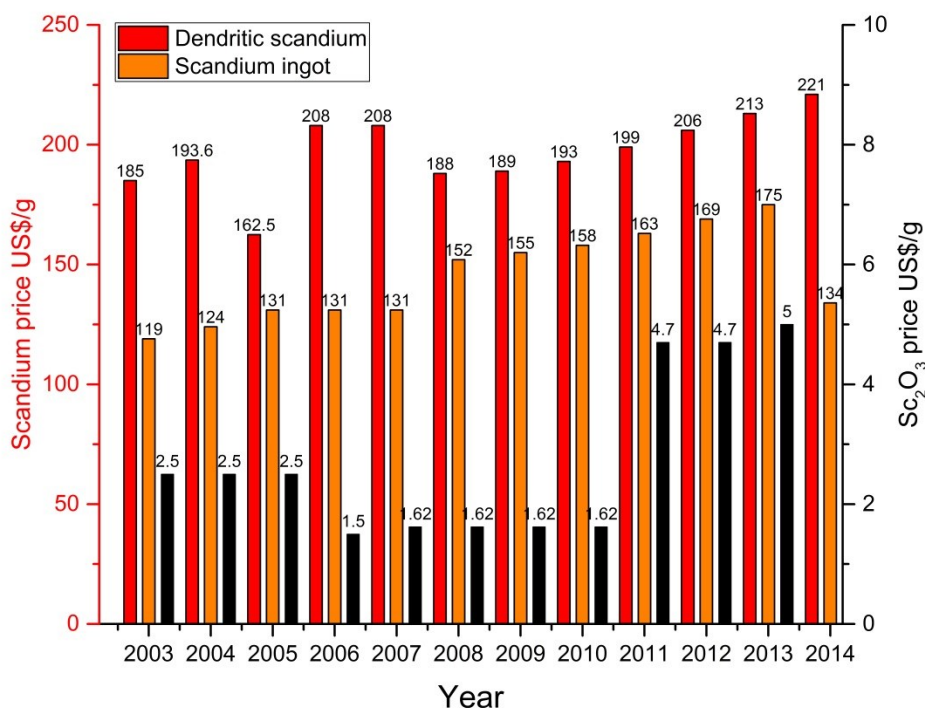
Figure 1.4. Scandium and Sc_2O_3 (99.99% purity) price in US$/g. Courtesy of U.S. Geological Survey, Mineral Commodity Summaries, years 2003-2014.

Ever since the first Sc-Al alloy was developed and marketed by Ashurst Technology Corporation for the construction of lightweight high-strength bicycle frames, many new applications for scandium-containing alloys have been proposed.[10] Since then, scandium steadily gained popularity as a small addition to both ceramic materials (in its Sc_2O_3 form) and alloys. Considering the scarcity of its supply it is not surprising that the price of dendritic scandium has been growing almost linearly over the last decade (see figure 1.4). While it is simplistic to directly relate the rise in scandium price to most recent metallurgical discoveries, it is still interesting to note that this increase is limited to dendritic scandium (often used as a starting material for alloys) and not to scandium ingots.

Over the last two decades the aircraft and space industries have become the most promising application fields for scandium. The use of Al–Mg–Sc alloys for aerospace guarantees low density (2.65 gcm^{-3}, which is three times lower than steel), high strength and a broad range of working temperatures (from -253 to +150 °C). Al–Mg–Sc alloys may reduce the weight of a construction by up to 15-30 % in comparison with common Al and Ti alloys, while ensuring better mechanical characteristics, thermal characteristics and chemical stability.

For all these reasons, in 2007 Airbus developed a new generation of Al–Mg–Sc alloys with the trade mark Scalmalloy®. This alloy shows good weldability and high joint strength and can be used for very high-strength extrusions, features which will be discussed in detail in the next section.

Furthermore, NASA recently tested Al–Sc alloys as material for fuel tanks and air frames for vehicles in which weight and compatibility with hydrogen peroxide is critical. Adding scandium and zirconium to aluminium alloys resulted in an increase in both mechanical properties and chemical stability and made those alloys suitable for H_2O_2 storage.[11]

Finally, significant efforts are being made to develop Sc-based master alloys for additive manufacturing.

1.4.1 Additive manufacturing

The production of net-shape components by additive manufacturing encompasses a wide range of materials via different fusion techniques. Many of the technologies are on a rapidly evolving path as a result of a wave of enthusiasm for 3D printing.[12] For the production of metallic components, these techniques range from powder-bed methods using optical lasers (Selective Laser Melting SLM, Selective Laser Sintering SLS, Direct Metal Laser Sintering DMLS …) and electron beams (Electron Beam Melting EBM) to sinter and fully melt metal powders, through to wire-based methods (Wire and Arc Additive Manufacturing – WAAM), Laser-Engineered Net Shaping (LENS) and Blown Powder and Direct Laser Deposition, all of which are reviewed by Frazier *et al.*[13] Each technique has its own benefits within a range of niche applications (higher build rates, lower surface roughness, lower porosity, larger component sizes, better geometrical tolerances, *etc*.), and arguably no single process is yet emerging clearly ahead of the others on a technical basis.[14]

While the range of printable materials is wide, the pallet of alloys ready for use with the available systems tends to be limited to mainstream and more standard alloy compositions.

The availability of alloys is partly determined by the accessibility of gas atomised powders, which are more readily available for the standard alloys. However, the rapid evolution of processes has also meant that the mainstream adoption of ALM-optimised metal alloys has been slower.

From the earliest production of significant quantities of scandium in the late 60s, scandium refined alloys were developed by the former Soviet Union scientists throughout the 70s and

80s to produce grain refined aluminium alloys, particularly for aerospace applications.[15] Dispersion of small Al_3Sc precipitates is encouraged by higher cooling rates as a result of supersaturation of Sc in Al (above 1%), well above the solubility limit of about 0.4%. This limits the effectiveness of Sc in aluminium alloys which require post-solidification heat treatment and/or processes with slower cooling rates such as casting.[16] On the other hand, scandium additions have been shown to be effective for processes with high cooling rates, such as fusion welding.[17] It is hardly surprising then that scandium additions have been looked at for use in SLM, where higher cooling rates make it possible to create hypereutectic Al–Sc alloys with up to 0.9%Sc.[18,19] Results show that the hypereutectic composition is retained during laser melting, resulting in high strength and good ductility parts. This has led to the first SLM specifically dedicated alloys: SCALMALLOY®RP, in Europe and PANDALLOY® in the US.[20,21]

2.   Scandium binary phase diagrams

The performance of scandium in combination with other metals or semi-metallic elements has been object of study ever since the 1960s and has led to the production of an extensive literature of binary and ternary phase diagrams. Out of the 97 possible binary phase diagrams (including stable lanthanides and actinides) the majority have been investigated either wholly or partially. These investigations were performed in inert atmosphere, starting from pure elements and mostly using induction furnaces (*e.g.* Sc–Sn, Sc–Pb, Sc–Cd, Sc–Zn phase diagrams) or arc-melting equipment (*e.g.* Sc–Au, Sc–Ru, Sc–Rh, Sc–In, Sc–Ir, Sc–Ni, Sc–Sn and Sc–Si phase diagrams).

The resulting data, collected from original papers and international databases (ASM and Springer Materials), are presented in figure 2.1 for reference in following sections. In the present review we have attempted to collect and evaluate experimental data effectively hidden in papers and PhD theses published in Russia and Ukraine to make this information accessible to a wider scientific community.

2.1 Scandium-containing binary systems and their classification

Knowledge of scandium binary and multicomponent phase diagrams and compounds is fragmented and requires critical analysis. Out of the 97 possible binary phases, 28 have never been explored (mainly non-metals but a few metals), 10 are covered only in partial composition and 9 other elements are only reported in ternary phase diagrams. As highlighted in figure 2.1, the currently reported binary phase diagrams can be divided into four types:

- Systems with complete mutual solubility in liquid and solid phase, in which no compounds occur (Type I);
- Systems with miscibility gaps in the liquid, in which no compounds occur (Type II);
- Systems dominated by a eutectic, with low mutual solubility in the solid phase and in which no compounds occur (Type III);
- Systems with at least one binary compound, with low mutual solubility in the solid phase (Type IV).

The first type includes Y, Zr, Hf, Nd, Gd and Tb. The second type comprises Li, Ca, Sr, Ba, Eu, Yb and U. The third type includes Ti, V, Cr, Mo, Ta, La, Ce, Er and Th. All other known binary phase diagrams (in complete or partial composition range) belong to the fourth type. The systematisation of scandium-based binary phase diagrams makes it possible to identify regularities and common trends.[22]
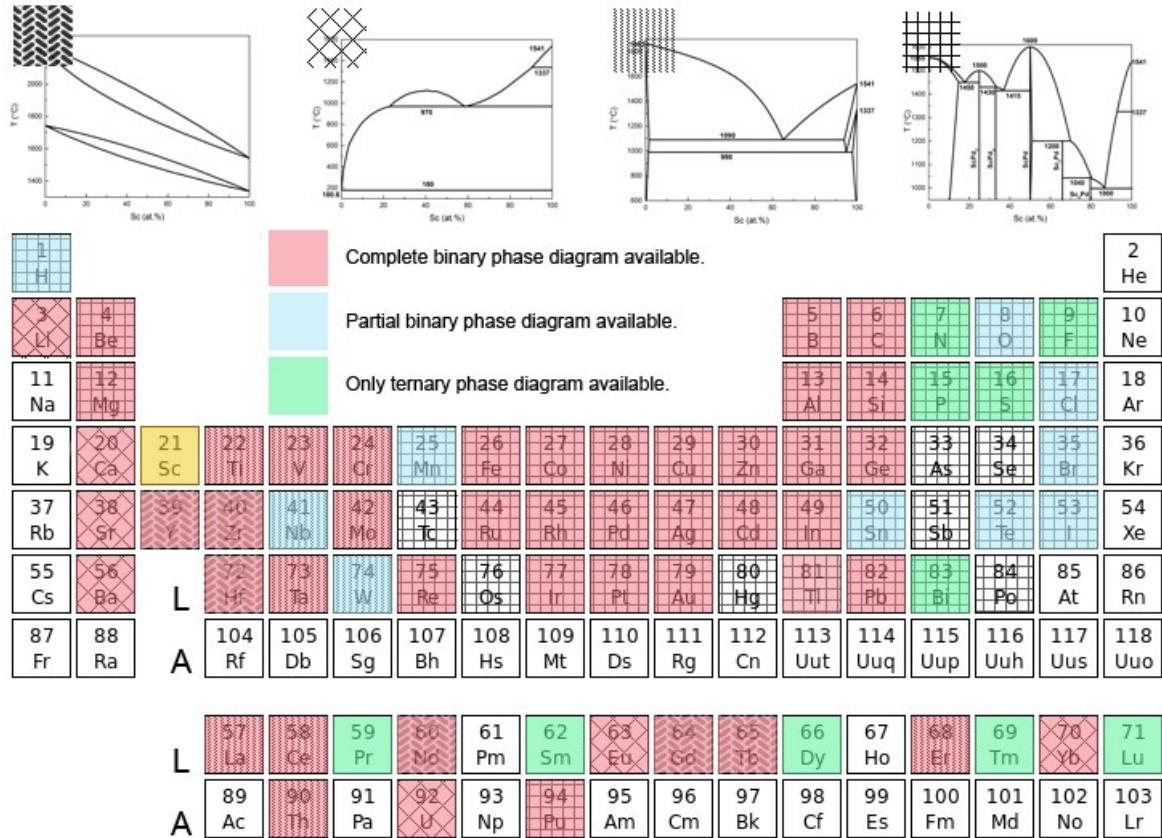
Figure 2.1 Scandium phase diagrams State of the Art. In red are phase diagrams studied over the whole composition range; in blue are binary phase diagrams covered only partially; in green are systems where information comes only from ternary phase diagrams; in white are currently unknown phase diagrams.

2.1.1 Systems with complete solubility in liquid and solid state (Type I)

Complete mutual solubility of scandium in Y, Zr and Hf (figure 2.1.1) can be easily related to their similar dimensions and electronegativities. Nevertheless, complete mutual solubility is also typical of scandium with other rare earths. It is worth noting that this behaviour is extremely unusual, and cannot be attributed to scandium's small atomic radius. In fact, even though both Zr and Hf have nearly the same atomic radius as Sc (1.602, 1.580 and 1.641 Å respectively), they generally form binary systems of the eutectic type with Y and lanthanides. On the other hand, it must be noted that several databases report Sc-Hf compounds, whose existence is in direct contrast with the binary phase diagram shown here. An experimental evaluation of the Sc-Hf phase diagram should be performed in more detail to confirm the existence of any binary and ternary compounds and their stability ranges.
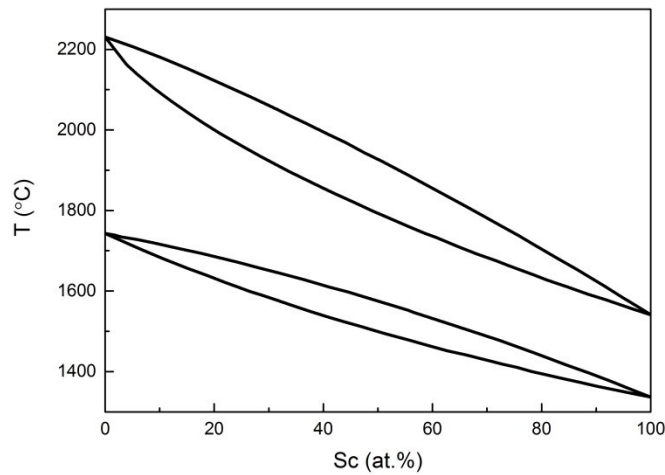
Figure 2.1.1. Sc−Hf phase diagram.[23]

2.1.2 Systems with a miscibility gap in liquid state and immiscibility in the solid state (Type II)

Among rare earths, only Eu and Yb have immiscibility in the liquid phase, probably due to the difference in valence between these elements (typically divalent) and scandium (trivalent). The divalent state is also a characteristic for alkaline earths and so it is not surprising to find that Ca, Sr and Ba binary phase diagrams all have immiscibility gaps in the liquid and the solid. The difference in valence, as well as electronegativity and melting temperature, is even more marked for alkaline metals. For Li group elements we can predict this same type of binary phase diagram (figure 2.1.2).
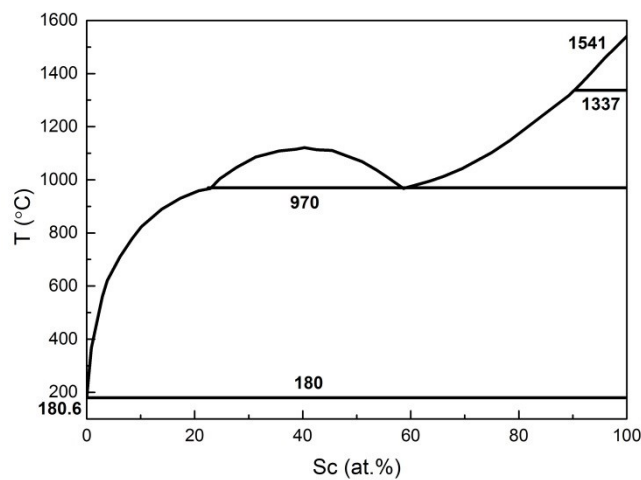
Figure 2.1.2. Sc−Li phase diagram.[24]

2.1.3 Systems with eutectic (Type III)

Scandium forms eutectic phase diagrams with Ti, La, Ce, Th and with V and Cr group elements. In general, moving towards elements of higher melting temperature causes a shift in the eutectic point towards the scandium melting point.

Comparing these systems, three trends can be identified:

- Sc forms eutectic only phase diagrams with Cr and Mo (figure 2.1.3.1),
- Sc forms a eutectic with a miscibility gap in the liquid phase with V, Nb and Ta (figure 2.1.3.1),
- Sc forms a eutectic with total miscibility in the liquid phase with Ti, La, Ce and Th (figure 2.1.3.2).
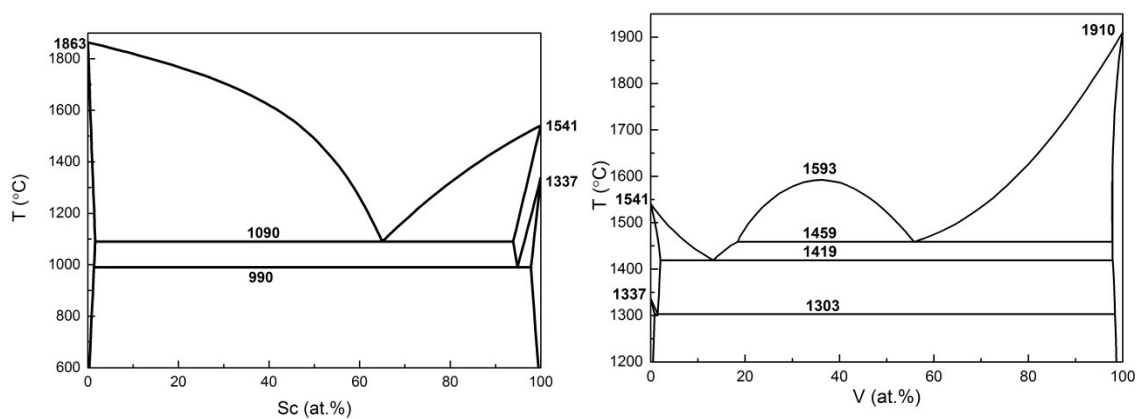

Figure 2.1.3.1. Sc–Cr (*left*) and Sc–V (*right*) binary phase diagrams.[24,25]
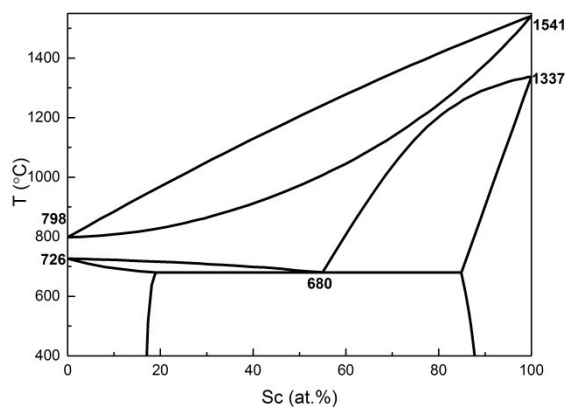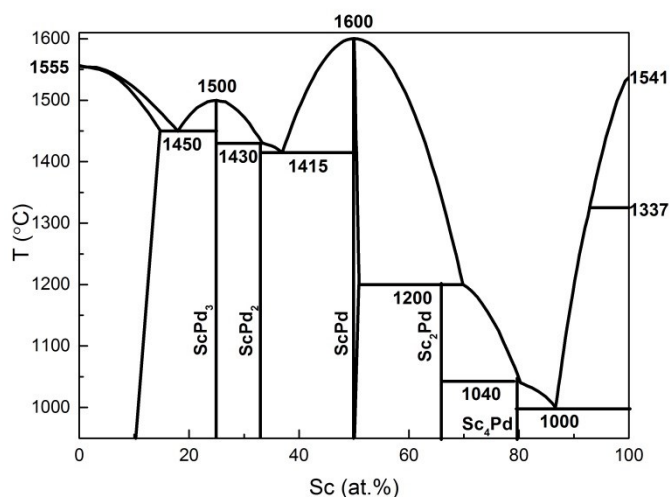

Figure 2.1.3.2. Sc–Ce binary phase diagram.[26]

2.1.4 Compound forming systems (Type IV)

All other metals, non-metals and metalloids create one or more binary compounds with scandium. In some cases (e.g. Hg, Os, Tc, As, Sb and Se) such intermetallics are known

despite the phase diagram not being investigated. The state of the art of scandium binary compounds will be reviewed and discussed in this section. The Sc–Pd binary phase diagram is shown in Figure 2.1.4 as a typical example of a compound forming Sc binary phase diagram.

Figure 2.1.4. Sc–Pd binary phase diagram.[27]

Iridium, ruthenium and thallium possess the maximum number of scandium intermetallic compounds (7). This makes the Ir–Sc, Ru–Sc, and Sc–Tl binary systems quite complicated for analysis and investigation. Also, the Sc–Tl phase diagram does not appear in common phase diagram databases and books. Nevertheless, it has been experimentally evaluated over the whole range of concentrations (Fig. 2.1.5).[28] The Sc–Tl phase diagram has two eutectic reactions in the Sc rich region at 1345 and 1450 K. The eutectic in the Tl rich region seems to be singular. Six compounds form via peritectic reactions and the Sc_5Tl_3 phase has the highest melting point at 1645 K. Sc_2Tl, Sc_5Tl_3, Sc_5Tl_4, ScTl and Sc_3Tl_5 compounds have been characterised structurally. Crystals of Sc_2Tl, Sc_5Tl_3 and Sc_5Tl_4 have hexagonal space groups $P6_3/mmc$, while Sc_3Tl_5 is orthorhombic, *Cmcm*. The powder diffraction pattern of ScTl can be possibly indexed in the cubic space group, but none of the structural types known for 1:1 intermetallic compounds fit the ScTl data. Sc_3Tl and $ScTl_2$ were proposed based on DSC data, but were not characterised in detail. Sc_5Tl_3 has an additional amount of Tl, which substitutes Sc in the structure. It has been concluded that this compound has a homogeneity range, increasing with increasing temperature. Its formula should therefore be written as

Sc_5Tl_{3+x} ($x = 0 \leq x \leq 0.85$). A more detailed investigation of the crystal structures and homogeneity ranges of Sc–Tl compounds is needed.
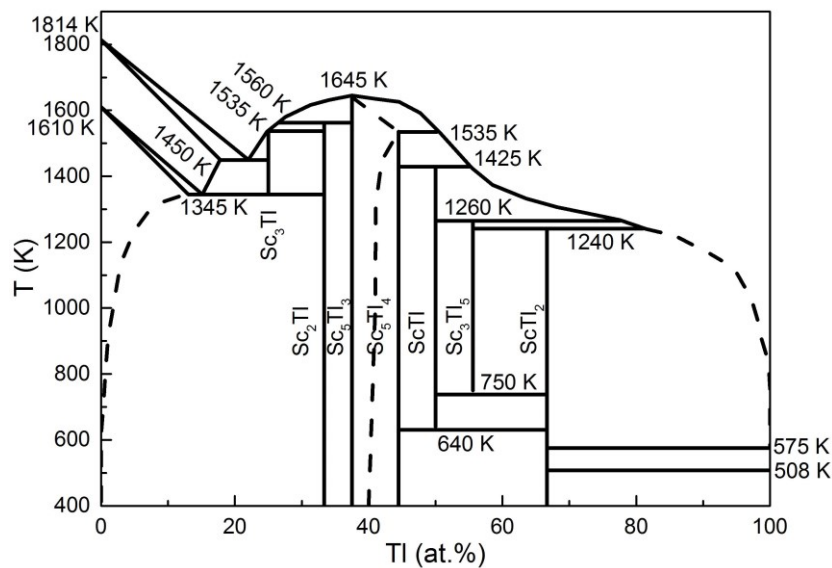
Figure 2.1.5. Sc–Tl binary phase diagram.[28]

2.2 Flaws and knowledge gaps

Not all of the known 68 (complete and partial) Sc binary phase diagrams can be considered as correct over the whole range of concentrations and temperatures. A number of thermodynamically unlikely features can be identified in published experimental diagrams. Okamoto and Massalski analysed existing experimental phase diagrams to stress all major flaws and highlighted the need for more careful experimental investigation and theoretical analysis.[29]

Table 2.2.1 summarizes those binary systems with problems according to Okamoto and our analysis of recent data. Several phase diagrams require reinvestigation and careful reassessment.

The main problems in the construction of these phase diagrams arise in the liquid region due to the relatively high melting temperatures. In many diagrams the liquidus lines are too flat or have incorrect shapes due to changes of slope. For example, $L_2+\alpha$(Sc) (figure 2.1.4), L+(V), and (Pd)+L boundaries should have positive convexity instead of negative.

Table 2.2.1. Problematic phase diagrams of binary systems.

Binary system	Unlikely futures
Hf-Sc	Controversial information about compound

	formation and number
<u>Sc-Tl</u>	Controversial information about compound number (see section 3)
Sc-Si (L+α-Sc)	Liquidus and solidus are not closing at zero at.% solute
Sc-W (W) Cr-Sc (Cr) Fe-Sc (β-Sc)	Too flat a liquidus
Fe-Sc (β-Sc+α-Sc/α-Sc)	Too steep a solvus
Pu-Sc (δ-Pu/δ-Pu+γ-Pu)	Too flat a solvus
Re-Sc (β-Sc)	Too steep a liquidus
Er-Sc (β-Sc) Er-Sc (β-Sc+Er/α-Sc)	Too wide a liquidus/solidus opening Too wide a solidus phase boundary opening
Sc-Th (α-Th+α-Sc) In-Sc: (α-Sc+Sc$_3$In,Sc$_5$In$_3$,ScIn+ScIn); (β-Sc+Sc$_3$In); (β-Sc/β-Sc+Sc$_3$In); (α-Sc/α-Sc+Sc$_3$In)	Two boundaries tending to cross one another
In-Sc (Sc$_5$In$_3$)	Compounds currently melting at off-stoichiometric composition
Ni-Sc (NiSc$_2$) Sc-Si (Sc$_5$Si$_3$) Al-Sc	Too asymmetric a liquidus
Al-Sc	Slopes of β-Sc solidus and α-Sc solidus cannot be similar
Mg-Sc	Two-phase field widening at higher temperatures
Cu-Sc	Compounds with a very flat liquidus
Sc-V	Unlikely thermodynamic model

Probably, the most important Sc phase diagram is the Al–Sc binary. Its existing equilibrium data have been already critically analysed to evaluate and improve known flaws and thermodynamically impossible features.[30,31]

As described above, alkali metals (AM) do not form intermetallic compounds with Sc. Due to the high difference in melting points between Sc and AM only the Sc–Li phase diagram has been experimentally investigated. These metals show extremely low mutual solubility in the solid state and almost no miscibility (L_1+L_2) in liquid state. However, the diagram is not complete for the Sc-rich region where the line of ternary equilibrium $L_2 \rightarrow L_1+\alpha(Sc)$ touches pure Sc at zero at.%.

In the Be–Sc and Mg–Sc binary systems several intermetallic compounds were found. Heavy Alkali-Earth metals (AE) with Sc show low mutual solubility in the solid and liquid states. High-temperature miscibility in the liquid state for Sc–AE binaries should be investigated in more detail, as should extreme temperatures for L_1+L_2 miscibilities. Be–Sc and Mg–Sc have several unlikely thermodynamic features in the solid state are most likely associated with low quality experimental data. The Mg–Sc phase diagram should be reinvestigated due to its importance in the design of lightweight Sc–Al–Mg alloys.

The V and Ta binaries with Sc show miscibility in the liquid phase and can probably be considered as complete and correct. Nevertheless, early experimental works considered both binaries as systems with a eutectic without miscibility in the liquid phase. After recent reinvestigation, both diagrams have been improved, especially in the liquid phase. The latest diagrams have L_1+L_2 miscibility below 1700°C.

The Sc–Nb phase diagram was originally considered as a system with eutectic. Extrapolating V and Ta phase diagrams to the Nb–Sc binary, one could assume that the Nb–Sc phase diagram should also have miscibility in the liquid phase and should probably be reinvestigated above melting temperatures to prove the presence or absence of L_1+L_2 miscibility.

The same situation applies for the next sub-group (Cr, Mo and W). The Cr and Mo binary systems with Sc show eutectic reactions. The impossible shape of the L+(Mo/Cr) boundaries should be considered incorrect and reinvestigated. The Sc–W phase diagram has been investigated only below 2000 K and the particular shape of L+W boundary has only been drawn approximately.

The Mn-subgroup (Mn, Tc and Re) has been barely investigated. Only the Re–Sc phase diagram data are detailed. The Sc–Tc phase diagram is still unknown and only a single ScTc

compound has been described in the literature. The Mn−Sc phase diagram has been investigated only for the Mn-rich side and should be considered as only partially known since at least one compound (Mn_2Sc) has been reported in the literature. The stability and equilibrium of the Mn_2Sc compound requires more study.

The Sc−Os, Sc−Hg and Sc−Tl phase diagrams have not been described in the literature. Nevertheless, a number of Sc−Os and Sc−Hg compounds were synthesized by direct melting. The appearance of Sc−Os and Sc−Hg compounds (as well as likely Sc−Tl intermetallics) enables us to place unknown phase diagrams together with compounds forming binaries, such as Fe−Sc, Co−Sc and Cu−Sc.

Only one third of Sc binaries with actinides and lanthanides have been investigated experimentally. Phase diagrams with Pr, Pm, Sm, Dy, Ho, Tm, Lu and Ac should be studied to finalize our knowledge on the general trends in Sc equilibriums with lanthanides and actinides.

To summarise, for Sc binary systems, there are many experimental errors and inaccuracies in the existing phase diagrams, as well as a number of unknown binaries. While many phase diagrams have only minor flaws and could easily be corrected, several phase diagrams are still only partially known (Mn−Sc, Sc−Nb, Sc−Ni, Sc with lanthanides and actinides) or completely unknown (Sc with Alkali metals, Sc−Os, Sc−Tc). Efforts should be made to reinvestigate Mg−Sc, Mn−Sc and Sc−Ni phase diagrams, since these binaries play important roles in the phase formation and properties of Sc-based multicomponent alloys.

3.   Scandium binary intermetallic phases

Current applications of scandium in the aerospace industry rely on solid solutions or precipitation hardening alloys whose performances are often enhanced by the presence of intermetallic inclusions. While intermetallic compounds offer superior mechanical properties and corrosion resistance (see section 5), their inherent brittleness has always represented a serious drawback.

However, in 2003 Gschneidner *et al.* discovered a new class of ductile binary intermetallic compounds of the B2 CsCl-type structure. Their particular features may open the way to the development of a new generation of alloys.[32]

The great majority of these ductile intermetallics contain either yttrium or scandium, and in particular: ScNi, ScPd, PcPt, ScCu, ScAg and ScAu. On the other hand, ScRu, ScCo, ScRh and ScIr are known to be brittle. A systematic study of scandium binary is needed to map out the interesting ductile intermetallic combinations.

Moreover, the outstanding effects of scandium additions on mechanical properties of multicomponent alloys reside in the formation of binary and ternary intermetallic compounds (see sections 4, 5 and 6). It is therefore of the utmost importance to known which compounds are likely to form in each system and if their symmetry is compatible with the alloy matrix. This information is reported below and in the Supplementary Information section.

Legend:
- 3 3 / Be box: Number of binary compounds in the system (Kotur, 1998). / Number of binary compounds in the system (this review).
- At least one compound has polimorphs.
- At least one compound with homogeneity range.
- At least one compound was found at high pressure.

Element	Kotur 1998	this review
H	4	n/a
Be	3	3
Mg	4	1
B	3	2
C	8	3
N	1	n/a
O	2	n/a
F	1	n/a
Al	4	4
Si	3	3
P	4	4
S	3	n/a
Cl	5	n/a
Mn	1	1
Fe	3	3
Co	4	4
Ni	5	5
Cu	3	3
Zn	6	5
Ga	6	8
Ge	5	5
As	4	3
Se	2	2
Br	1	n/a
Tc	2	5
Ru	7	4
Rh	5	5
Pd	6	5
Ag	3	3
Cd	3	3
In	5	6
Sn	5	4
Sb	3	3
Te	5	2
I	1	n/a
Hf	3	0
Re	2	2
Os	3	3
Ir	7	7
Pt	4	4
Au	6	4
Hg	2	2
Tl	7	7
Pb	2	2
Bi	2	1
Po	1	1
Pu	1	1

Figure 3.1. Overview of scandium binary intermetallics according to literature search and a 1998 paper from Kotur.[33]

Kotur gave an outstanding overview of crystal topology and formation tendencies in Sc-based intermetallics.[33] Up to now his review is the first and last systematic analysis of scandium binary and ternary alloys and compounds. As shown is figure 3.1, a total of 170 scandium binary compounds are known (against the 114 mentioned in the review by Kotur).[33] Most of them occur at constant composition, and only four compounds are known to have a homogeneity interval of 0.85-5% namely ScPd, Sc_5Tl_3, ScMg and ScC_{1-x}. Nevertheless, compounds with homogeneity ranges are reported in several binary phase diagrams e.g. Co_2Sc, Ni_2Sc, Ru_2Sc, RuSc, RhSc, Rh_3Sc, CdSc, IrSc, Ir_2Sc, $IrSc_2$ and Sc_2Ge_3.

Some binary compounds occur in two ($ScFe_2$, $ScNi_5$, Sc_4C_3, Sc_3Si_5, Sc_3P_2) or three (Sc_3As_2) polymorphic modifications whose crystal structures are structurally related. Some compounds display magnetic transitions at high temperatures which result in a change in symmetry ($ScFe_2$, Sc_2S_3).

The comparison between our and Kotur's overviews highlight the interest raised by scandium compounds. Sc intermetallics with non-metal elements in particular have been extensively studied in the last fifteen years. Nevertheless, in some cases the opposite trend occurs. Thus several compounds of scandium with Tc, Ga and In are not available in most common databases.

Finally, it is worth noting that scandium forms three binary compounds with Hf. This is in direct contrast with the Sc-Hf phase diagrams, which display no compounds and total solubility of the metals in both the solid and liquid phases.

3.1 Synthetic pathways

A great number of intermetallic phases can be produced starting from two or more pure elements. Suitable methods for achieving pure, stable compounds differ. It is important to take into account each species' melting behaviour, the number of intermediate phases, eventual formation of solid solutions, *etc*.

Direct melting is the most popular technique for achieving binary compounds. Despite its simplicity melting has some limitations. If an alloy is cooled too fast, a non-equilibrium phase is created and subsequent treatments are needed in order to achieve a homogeneous sample. Moreover, some compounds may be difficult or impossible to synthesize with this method, for example when the melting temperature of one component is higher than the boiling point of the other. In this latter case it may be worth considering less drastic approaches, such as interface diffusion.

During interface diffusion processes two metals are placed in contact with one another and heated up to the melting temperature of the lower-melting point species. The melted metal will slowly diffuse through the interface and react with the other metal. Several re-melting steps are usually necessary to obtain a homogeneous sample. This method has gained popularity in the framework of high-throughput metallurgy (the Diffusion-Multiple Approach).[34,35]

Many scandium binary and ternary compounds were investigated using powder and single-crystal X-ray diffraction. Their magnetic properties were characterised by susceptibility curves. Their thermodynamic properties and stability were measured using DSC. Scandium intermetallic compounds can also be successfully characterized by solid-state NMR spectroscopy. ^{45}Sc isotope with I = 7/2 has 100 % natural abundance and excellent characteristics for investigations based on the NMR technique. Recent papers reporting the correlation of the ^{45}Sc NMR parameters with local structural data in intermetallic compounds have been reviewed by Eckert and Pöttgen.[36] It has been demonstrated that local site symmetry, site multiplicity and defects can be successfully characterized in stoichiometric and non-stoichiometric intermetallic systems as well as their temperature- and composition-dependent phase transitions.

3.2 Scandium binary compounds: state of the art

Crystal chemistry, structures and general trends in scandium intermetallic compounds have been summarised in a number of detailed reviews.[22,33,37]

An overview of known scandium binary compounds as well as crystal structure and formation enthalpy can be found in the Supplementary Information. The corresponding references are included in the main bibliography.[8,28,38-78]

Crystallographic and structural information derive from the ICSD international database, while formation enthalpies are taken from selected papers. Acquisition methods vary between compounds (and for the same compound).

Trends in stability, recurring and less-ordinary structures will be highlighted in the next sections. Many potential future applications for Sc (*e.g.* thermoelectric materials and superconductors) require anisotropic crystals and peculiar symmetries. Some of the many complex structures typical for Sc intermetallic compounds are thus described.

3.2.1 Recurring and non-ordinary crystal structures

As shown in Table 1 of the Supplementary Information, scandium intermetallics with a given element 'E' often occur at stoichiometries ScE, ScE_2, ScE_3, Sc_2E and Sc_5E_3. Depending on the electronegativity, electron concentration and atomic size of the element E, compounds crystallise in different structure types.

The most common crystal structures for ScE are $Pm\bar{3}m$ (CsCl-type) and $Fm\bar{3}m$ (NaCl-type) if E is a metal, or $Fm\bar{3}m$, when E is a non-metal. In the former each Sc atom is surrounded by 8 neighbour E-atoms forming a cubic polyhedron. For NaCl-type structures each atom has 6 neighbours forming an octahedral polyhedron. These two crystal types (CsCl and NaCl) are the most common for 1:1 intermetallic compounds along the periodic table and have been described in detail elsewhere.
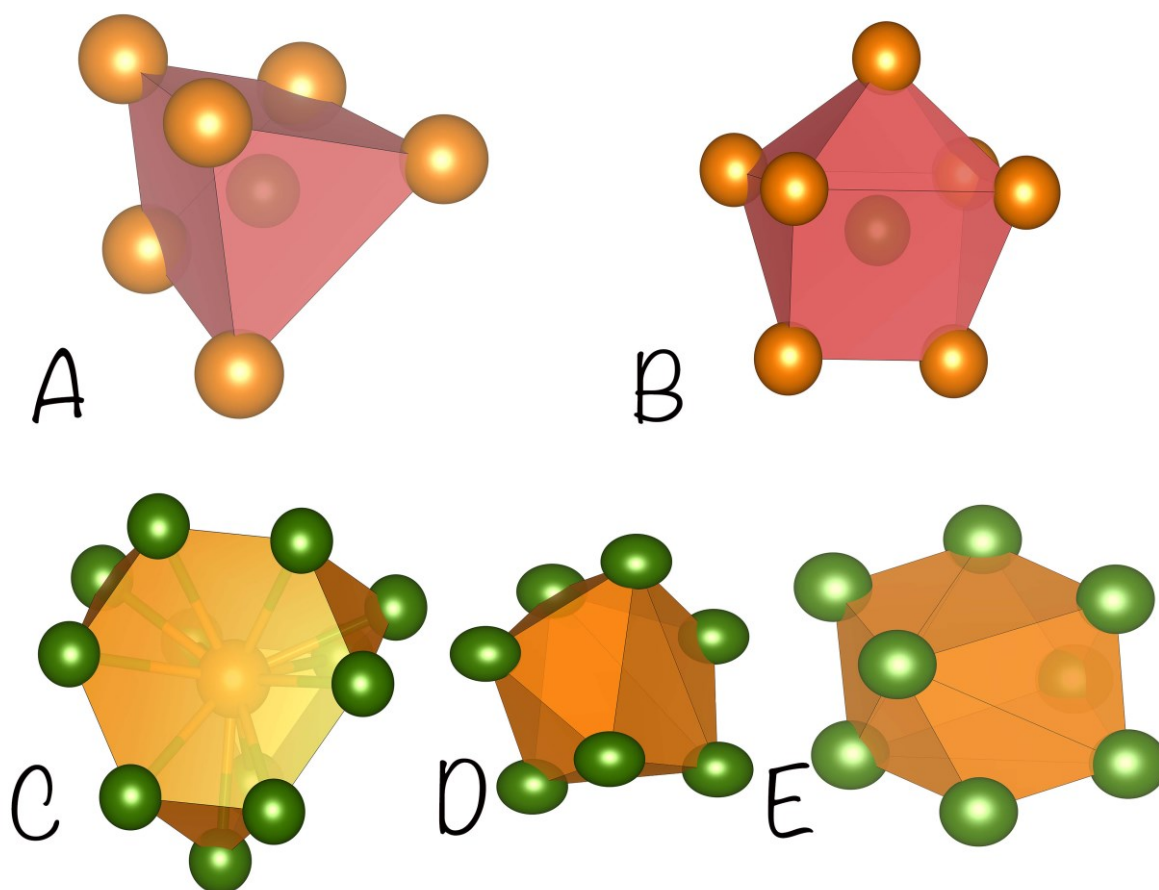
Figure 3.2.1. Polyhedra for $ScIr_6$ (in the crystal structure of $IrSc_2$), $ScSn_7$ (in the crystal structure of Sc_5Sn_3), $ScIr_{12}$ (in the crystal structure of Sc_2Ir), $RhSc_7$ (in the crystal structure of $Sc_{57}Rh_{13}$), and $IrSc_8$ (in the crystal structure of $Sc_{44}Ir_7$).

ScE_2 compounds crystallise in a variety of space groups and crystal types. The most common are the close-packed MgZn$_2$, MgCu$_2$ and MgNi$_2$ types. Many crystal structures can be found in two space groups $Fd\bar{3}m$ (for example, Ir$_2$Sc and other originally fcc metals such as Co, Pt, and Pd) and $P6_3/mmc$ (for example, Re$_2$Sc and other hcp metals such as Mn, Tc, Ru, In). Both crystal structures can be described as ordered cubic or hexagonal closed packing of E and Sc atoms. Sc and the second element form the same closed packed structure and in principle can form partially disordered phases depending on the temperature and composition. In both crystal structures, each Sc atom has 12 neighbouring atoms, as required by fcc- and hcp-structured alloys.

In a few rare crystal structures, Sc forms polyhedra of low local symmetry. For example, the cubic structure of IrSc$_2$ has a much bigger elemental cell in comparison with Ir$_2$Sc. Each Sc atom has 6 Ir neighbouring atoms which form a trigonal prism. The orthorhombic structure of PtSc$_2$ (together with CoSc$_2$) has a trigonal prism with a centred face as a coordination polyhedron for Sc atoms (figure 3.2.1).

The Sn-Sc binary system gives a unique layered structure of tetragonal ScSn$_2$ (figure 3.2.2). The crystal structure consists of 12 layers along the c-axis. A flat Sn layer follows after two mixed layers where equal numbers of Sc and Sn atoms form deformed zigzag sequences. The Sc/Sn layers have different atomic arrangements in which Sc-Sn and Sc-Sc/Sn-Sn pairs can be found.
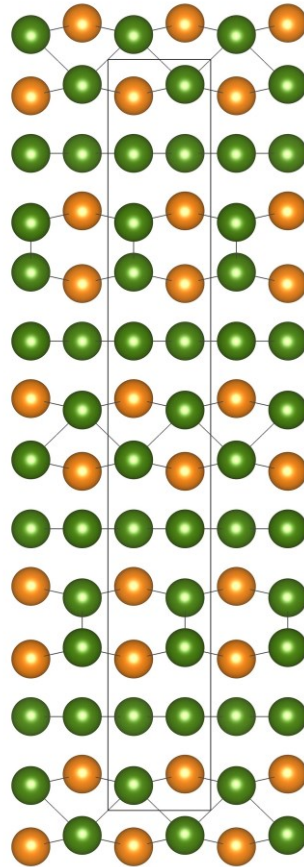
Figure 3.2.2. $ScSn_2$ crystal structure ($I4/amd$ space group) along a-axis (orange spheres represent Sc and green spheres represent Sn).

ScE_3 compounds crystallise as $AuCu_3$ or $SnNi_3$-types. In the Rh_3Sc crystal structure, the bigger Rh atoms form face-centred close packing with the smaller Sc atoms in octahedral cavities. In principle it is possible to form Sc_3E intermetallics in which E atoms are smaller in comparison with Sc atoms, but this situation is quite rare.

Several scandium binary compounds crystallise in the Sc_2E stoichiometry, mainly as Ti_2Ni and Al_2Cu structure types. Finally, Sc_5E_3 pnictide compounds crystallise as Mn_5Si_3 and Yb_5Sb_3 structure types.

While the stoichiometries ScE, ScE_2, ScE_3, Sc_2E and Sc_5E_3 represent the most common scandium binary compounds it is also true that some trends emerge inside one group, or between elements with diagonal relationships. Between these structures ScE_4 and $Sc_{11}E_4$ appear quite frequently and display a high order of symmetry and complexity. The crystal structure solved for $ScAu_4$ (figure 3.2.3) can be described as a body centred cubic arrangement of Sc atoms. Each Sc atom has 8 neighbour Au atoms forming ideal cubes with

2.8926 Å Sc-Au distances. Cubes share opposite faces and form columns along the *c*-axis. This crystal structure has tetragonal symmetry and can be characterized by a relatively high packing density. In the similar crystal structure of $ScAu_2$ (as well as Cu and Ag analogues) the Sc atoms can be found in a body centred tetragonal cell with 8 Au neighbour atoms forming cubes as coordination polyhedrons with 2.8709 Å Sc-Au distances. $ScAu_8$ cubes form isolated layers where each cube shares 4 faces with neighbouring polyhedra.
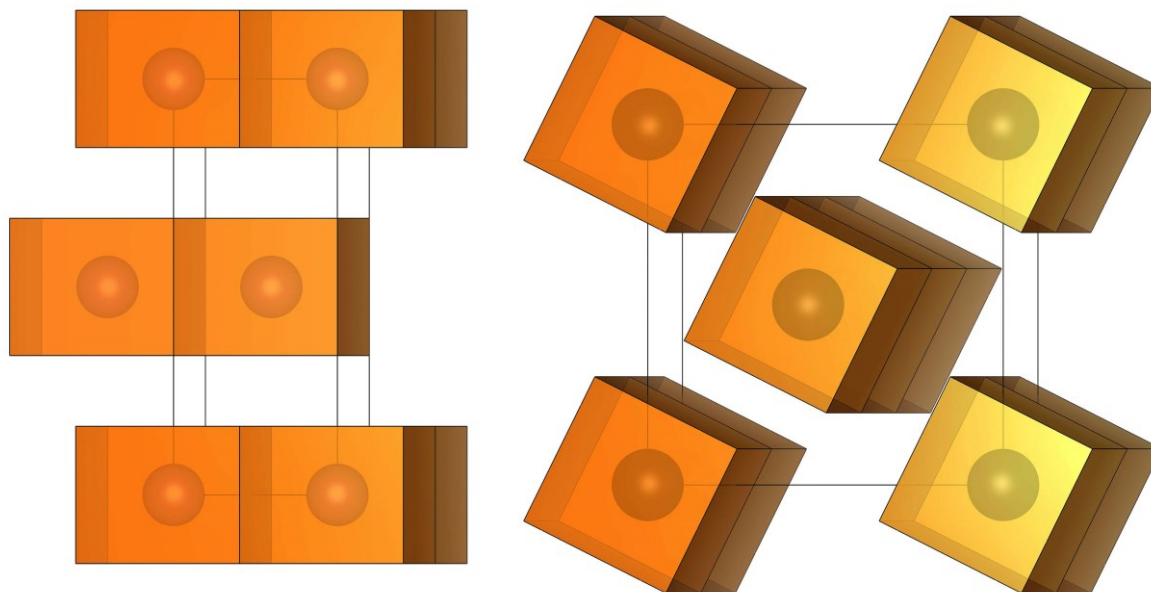

Figure 3.2.3. Polyhedral representation of crystal structures of the Au_2Sc crystal structure along the *a*-axis (*I4/mmm* space group, *left*) and Au_4Sc along the *c*-axis (*I4/m* space group, *right*) (Sc polyhedra are shown).

Compounds of the $Sc_{11}E_4$ type have been described using the cluster approach. Their crystal structures relate to that of Th_6Mn_{23} but with additional atoms located in four octahedral positions. The crystal structure of $Sc_{11}Ir_4$ (figure 3.2.4) consists of $IrSc_4$ planar squares which form an interconnected cubic framework with open channels along the *a*-, *b*- and *c*-axes. Channels are filled with cubic and octahedral clusters of $IrSc_8$ and $IrSc_6$. Ir-Sc distances are 2.698 and 2.663 Å for $IrSc_8$ and $IrSc_6$ respectively. Both clusters form NaCl-type packing inside channels. More complex intermetallics with the formula $Sc_{44}Ir_7$ show rare $IrSc_8$ deformed cubes as main coordination polyhedra for Sc (figure 3.2.4).
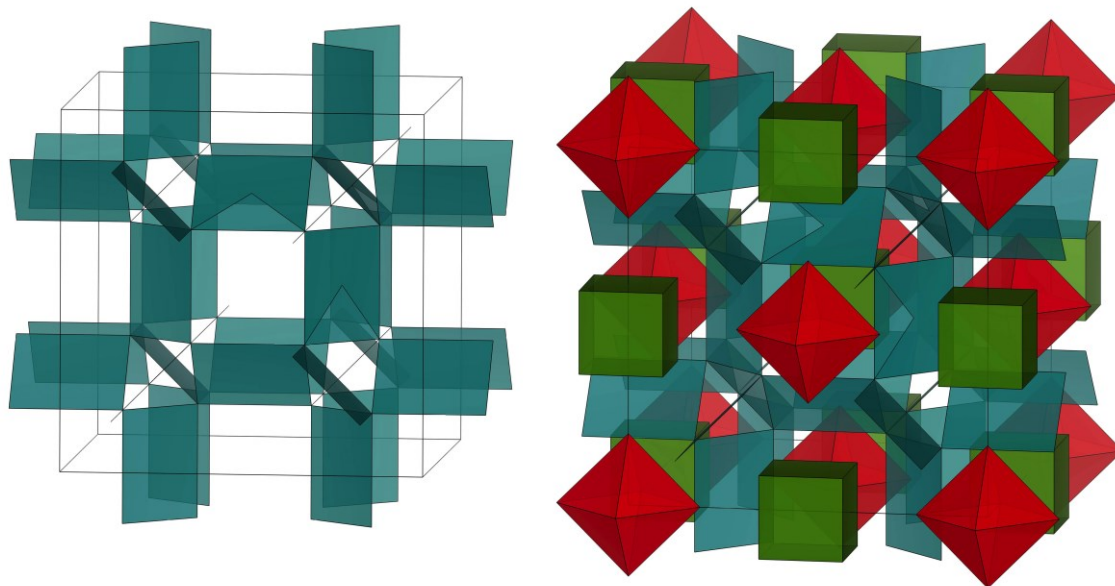
**Figure 3.2.4.** Fragment of Ir_4Sc_{11} crystal stracture (*left*) showing interconnected $IrSc_4$ planar squares ($Fm\bar{3}m$ space group) and the complete structure (*right*) along the *c*-axis.

The formation of partially disordered structures and polymorphic modifications is quite rare among Sc intermetallics. $ScFe_2$ and $ScNi_5$ have been mentioned as compounds with temperature dependent polymorphism. According to Kotur, Fe_2Sc has three polymorphic modifications: α-Fe_2Sc ($P6_3/mmc$, $MgZn_2$ Laves phase), β-Fe_2Sc ($P6_3/mmc$, $MgNi_2$ phase) and γ-Fe_2Sc ($Fd\bar{3}mS$, Cu_2Mg Laves phase).[79,80] The α → β transformation in Fe_2Sc occurs above 1565 °C. Below 1200 °C, with Sc content close to 36.5 at.%, β- and off-stoichiometric γ-Fe_2Sc phases are in equilibrium (figure 3.2.5). In the series Mn-Fe-Co-Ni, Mn_2Sc forms a Mg_2Zn structure and Co and Ni form a $MgNi_2$ structure. The intermediate position of iron suggests the appearance of both crystal types and polymorphism in Fe-Sc compounds.[81]
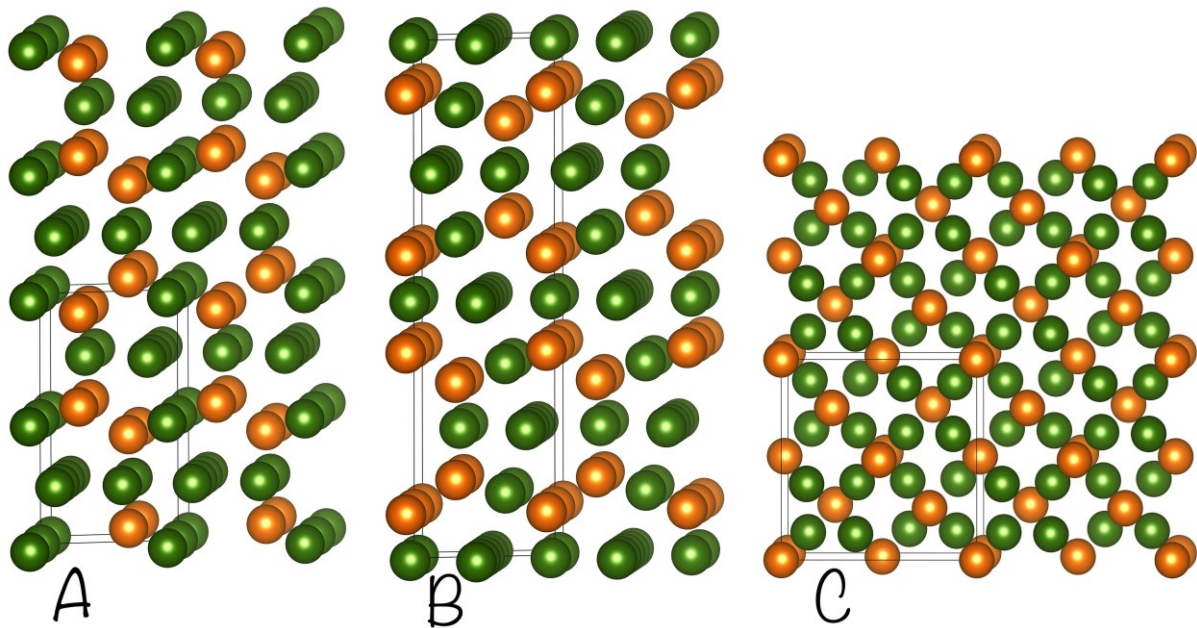
Figure 3.2.5. α-, β- and γ-Fe$_2$Se along the *c*-axis (green spheres represent Fe atoms, orange spheres represent Sc).

The Sc–Ni system has been investigated for Ni-rich compositions.[82,83] In the first experimental work performed by Goebel and Rosen, temperature dependent phase transitions in ScNi$_5$ and Sc$_2$Ni$_7$ have been proposed.[84] A later work, however, showed no polymorphism in Sc$_2$Ni$_7$.[82] Room-temperature ScNi$_5$ phase has a narrow stability range and can be formed by peritectic reaction from hexagonal Sc$_2$Ni$_7$ at 1180 °C: *Liquid* (14.at.% Sc) + Sc$_2$Ni$_7$ = ScNi$_5$. Hexagonal Sc$_2$Ni$_7$ also has a narrow stability range and can be melted at 1295 °C. ScNi$_5$ at room temperature has hexagonal structure where Sc atoms occupy a primitive unit cell. Each Sc atom has 18 neighbouring Ni atoms. The Sc coordination polyhedron has 2 hexagonal, 6x2=12 triangular and 6 squared faces (figure 3.2.6). This coordination polyhedron is quite unusual for an intermetallic compound. The compound does not decompose with formation of other phases and instead undergoes phase transition at 880-900 °C with the formation of a low-symmetry structure. The detailed crystal structure has not been determined and only monoclinic or triclinic crystal systems have been proposed.[82]
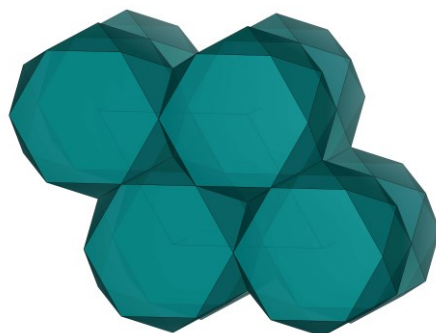
Figure 3.2.6. Ni_5Sc crystal structure (*P6/mmm* space group).

To summarise, Sc binary intermetallics show a large variety of stoichiometries, symmetries and possible coordination polyhedra. Many crystal structures such as Ru_3Sc_5, Cu_4Sc, $PdSc_4$ are still unknown. Sc has a relatively small metallic radius and can form not only closed packed ordered and disordered structures but also cluster-based compounds with Ir, Cu, Ag and Au with cubically coordinated Sc centres. The appearance of polymorphism in the Sc–Ni binary system should be taken into account with respect to temperature dependent modifications in other binaries and ternaries of scandium with transition metals.

3.3 Stability

The table reported in the Supplementary Information gives an overview of the formation enthalpy of several scandium intermetallic compounds. The formation and stability of intermetallic compounds of different structure and stoichiometry is strictly linked to atomic size, electron concentration (defined as the ratio between the number of valence electrons and total number of atoms in the unit cell) and electronegativity. Atomic size plays an important role in the relative solubility in the solid state of different systems whereas a high difference in electronegativity implies a high probability of stable intermetallic compounds (Hume-Rothery's first and second rules). Finally, electron concentration influences both solid-state solubility and stability of intermediate phases (Hume-Rothery's third rule). The formation of stable compounds is favoured by the filling of the valence shell of one of the atoms of the compound.

All these criteria participate in the stability of the **equiatomic Sc*E* phase**, which occurs in the great majority of scandium compounds. Elements that form this phase are distributed almost symmetrically with respect to the Cr group (whose elements do not participate in the formation of such compounds). First, the difference between interatomic distance (D_{AB}) and

distance between atoms in the compounds (d_{AB}) in the lattice of CsCl phases is correlated to the stability of the compound. Accordingly, the stability of equiatomic scandium compounds increases along a group and decreases along a period. The electron concentration also plays a role. The optimal interval of *e/a* for the formation of CsCl phase has been calculated as 5.5-7.0, and contains all known scandium equiatomic compounds.

Finally, depending on *d* spin and orbital contributions, scandium CsCl compounds can be divided into three groups, as the Fermi level moves from the Sc dominated *d* region (Group 1, comprising ScCu, ScAg and ScPd) towards the *d* band of the partner element with lower energy (Group 2, ScRu), passing a region of possible overlapping *d*-bands (Group 3, ScIr and ScRh). Group 1 relates to a larger orbital contribution arising from Sc, and therefore total orbital contribution and spin are disproportionately allocated. Group 2 corresponds to the opposite situation. Group 3 arises if the contribution of both elements is small.[85]

The **ScE_2 Laves phase** consist mainly of hexagonal and *fcc* structures. It is worth noting that most of the scandium compounds of these classes have the same syngony as the starting *E* element. For example, Os, Ru, Re and Zn, which have *hcp* symmetry, create hexagonal ScE_2 compounds. On the other hand, Pd, Ir, Ni and Al, which have *ccp* symmetry, create Laves phases of *fcc* symmetry. Valid exceptions are Cu, Ag and Au: originally of *ccp* symmetry, they create a tetrahedral ScE_2 phase. Even though several efforts have been made towards the prediction of Laves phases, neither atomic radius, electronic concentration or electronegativity has been deemed a sufficient precondition for the occurrence of such a phase.

The size factor is central for the formation of the **ScE_3 phase**, favoured when the ratio between atomic radii is in the range 1.00-1.21. However, electron concentration is just as important, since this structure type principally arises when a group III-VI element (such as scandium) is combined with the VIII group element (rhodium or iridium).

The interaction of Sc with group VIII metals also favours the **Sc$_2E$ phase**. The high formation enthalpy of Sc_2Pd, Sc_2Pt and Sc_2Rh, similar in structure to the so-called high-speed steel carbide Fe_3W_3C, is related to the presence of oxygen, nitrogen or carbon impurities acting as stabilizers. The influence of electron concentration and atomic radii of the Sc_2E phase stability is very limited.

The stability of less recurring structures such as **Sc$_{11}E_4$**, **Sc$_{57}E_{13}$** and **Sc$_{44}E_7$** is not really explained using these concepts. The ambiguous behaviour of elements of the same group calls for more sophisticated approaches.[86]

**3.4 Scandium intermetallics under high-pressure**

Binary Sc intermetallics have been sporadically investigated under high-pressure. Only Sc–Zn and Sc–Ga binary compounds were investigated under moderate pressure. Three intermediate phases were found in the reaction between elemental Sc and Ga at 7.7 GPa in the temperature range 200 to 1000 °C: Sc_5Ga_3 (Mn_5Si_3 structure type), $ScGa_2$ ($ZrGa_2$ structure type), and $ScGa_3$ (Cu_3Au structure type) have been characterized. Only Sc_5Ga_3 is stable under ambient pressure. It has been noted that the Sc–Ga phase diagram becomes more complicated with increasing pressure. $ScGa_2$ exists at ambient pressure phase with an *Imma* space group and the high-pressure phase crystallizes as a *Cmmm* space group. The ambient pressure phase can be described as a Ga framework with hexagonal channels along the *b*-axis filled by Sc atoms (figure 3.4.1). The high-pressure phase can be described as two-layered close packing along the *a*-axis. Pure Ga layers follow sequentially mixed Sc and Ga (1:1) layers.
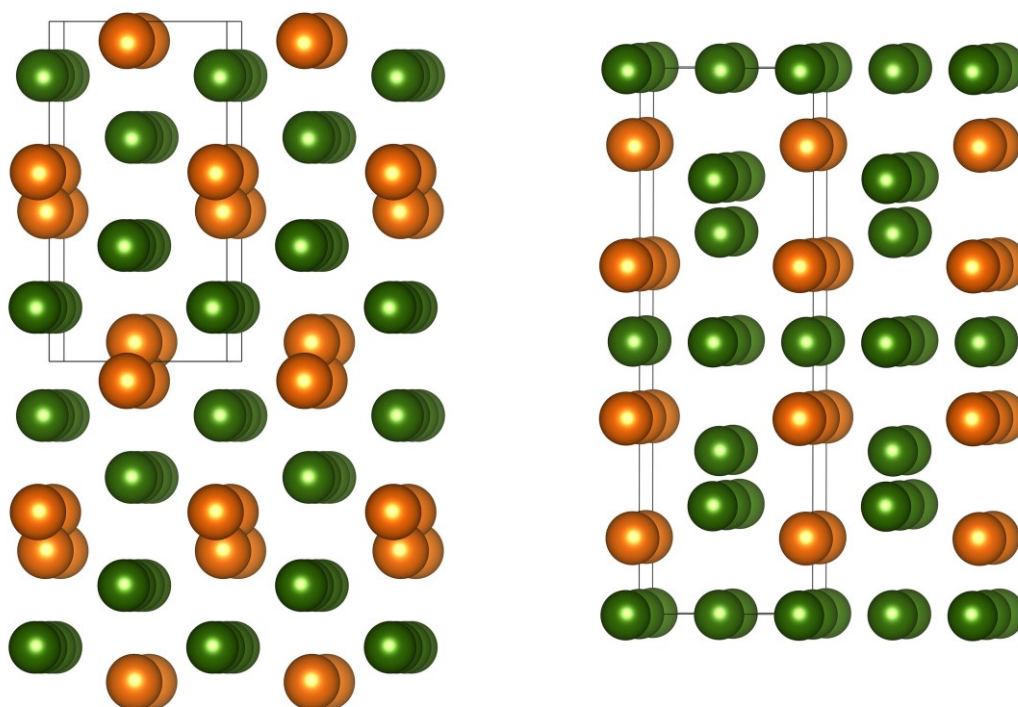
Figure 3.4.1. Ambient-pressure along *b*-axis (*left*) and high-pressure (*right*) phases of $ScGa_2$.

The reaction between elemental Sc and Zn at 4 GPa and 1900 °C results in the formation of hexagonal closed packed $ScZn_2$ phase (figure 3.4.2, a $MgZn_2$ structural type similar to many other ScE_2 intermetallics) which can be recovered after cooling the reaction apparatus and

decompressing.[87] $ScZn_2$ phase does not exist under ambient pressure (only $ScZn$, $ScZn_{12}$, and Sc_3Zn_{12} have been described in the literature).
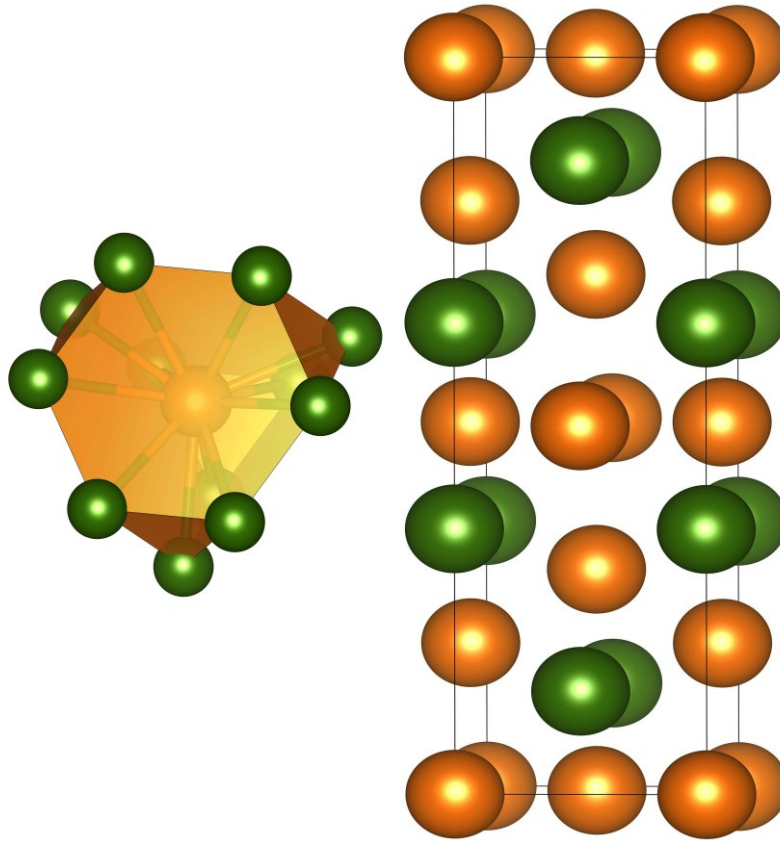
Figure 3.4.2. $ScZn_{12}$ coordination polyhedron (*left*) and high-pressure crystal structure of $ScZn_2$ (*right*).

4. Scandium ternary systems

In the last two decades efforts made in the study of scandium alloys have brought a massive increase in the amount of data available from international databases. While the first wave of interest in scandium intermetallics could be related to the superconducting properties of scandium ternary compounds of the $Sc_5M_4X_{10}$ series (where M is a transition metal of the Ni, Fe or Co group, and X is either Si or Ge - *i.e.* $Sc_5Co_4Si_{10}$), the renewed efforts in scandium development are undoubtedly linked to structural properties in multicomponent alloys.[88,89] The number of known scandium-containing ternary systems has increased from the roughly 100 known to Kotur in 1998 to over 200 (considering both partial and complete composition range) today.[33] Among these high importance has been given to the Sc–Al–X (33), Sc–Si–X (24), Sc–B–X (10), Sc–Ge–X (9), Sc–Fe–X (7) and Sc–C–X (6) systems. Simultaneously the number of synthesized ternary compounds has doubled, reaching over a thousand.

Kotur pointed out the regularity of the occurrence of a large number of compounds on some characteristic cross section of phase diagrams. In fact, many Sc–M–X intermetallics (M=Al, Si, B, Ge or C) occur at the following stoichiometries: Sc/X=1/1, Sc/M=1/1, M/X=1/1, Sc/X=1/2 and Sc/M=1/2. Therefore, the great majority of scandium compounds have composition ScMX, ScMX_2, ScM_2X and ScM_2X_2. Such simple stoichiometries are favoured by metallic bonding while structures of higher complexity appear in compounds with covalent bonding.

Moreover, scandium ternary compounds occur in the ternary system region where scandium content is equal to or lower than 50 at.%. In this case, scandium behaviour resembles that of d-elements, whereas light rare-earth intermetallics often occur at RE content greater than 50 at.%. The peculiar features of scandium in the framework of compound formation can be ascribed to the atomic size factor, which plays an important role in the distribution of atoms in the ternary phase. In particular, the larger atoms of the compound usually occupy sites with larger coordination number and *vice versa*. Scandium is generally the largest atom in the structures, unless other rare earths metals are included.[90]

While a complete overview of scandium ternary compounds falls outside the aims of this review, it is still worth describing a few systems of industrial importance in which scandium intermetallics play a major role.

4.1 Al–Cu–Sc: the W phase

Al-Cu-Sc-based multicomponent alloys were primarily investigated to develop hard and heat-treatable Al alloys. Kharakterova reports the existence of 9 ternary compounds in the Al−Cu−Sc ternary system, 3 of those located at the Al-rich corner of the phase diagram (AlCuSc, $AlCu_2Sc$ and $Al_{5.4-8}Cu_{6.6-4}Sc$). For the last compound a $MnTh_{12}$ –type crystal structure with lattice parameters a=8.63 and c=5.10 Å was estimated. Intermetallics similar to AlCuSc (namely AlCoSc and AlNiSc) with $MgZn_2$ structure ($P6_3/mmc$, $a = 5.04$, c=8.24 Å) were also described in the literature (see next section).[91]

The difficulties encountered in the characterisation of these phases resides in the stability range broadening of the three-phase areas while decreasing temperature.[92]

More recently, several authors have noted that the formation of the so-called *W phase* (i.e. the ternary AlCuSc phase) significantly influences the properties of these alloys. Various compositions have been proposed for the W-phase: $Al_{5-8}Cu_{7-4}Sc$, $Al_{5.4-8}Cu_{6.6-4}Sc$ and $Al_{8-x}Cu_{4+x}Sc$, with a possible $I4/mmm$ crystal structure similar to Al_2Cu. Nevertheless, only a few detailed investigations have been carried out to clarify the ternary phase structure and occurrence.

In general it has been noted that the formation of the W phase in Al alloys is unfavourable. The formation of the W-phase consumes part of the Sc and Cu atoms embedded in the Al matrix. As a consequence, both the precipitation of Al_3Sc and the occurrence of Cu strengthening phases are reduced and this minimises the positive effect of Sc on the mechanical properties of the alloy.[93]

This overall negative effect is somewhat surprising considering the W-phase microhardness (5150-5700 MPa) is higher than Al_3Sc (3900-4300 MPa) and Al_2Cu (4400-5000 MPa).[92]
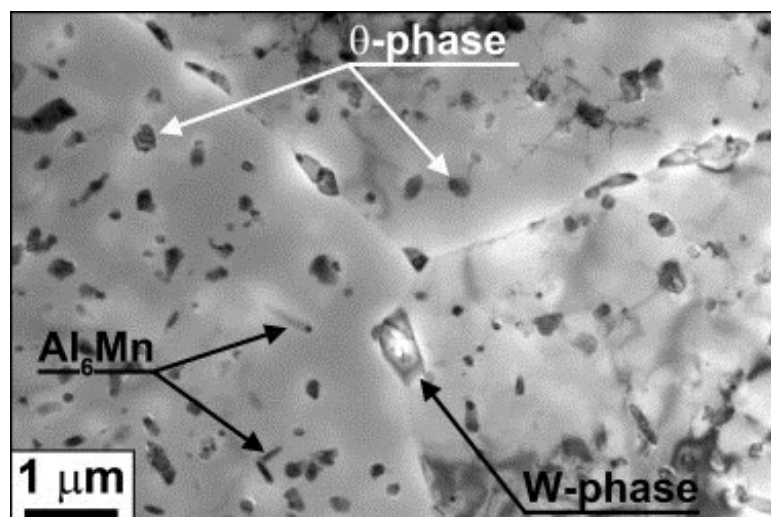
Figure 4.1.1. Representative structure of Ag–Al–Cu–Mg alloy with Sc addition observed by bright-field TEM.[94]

The W-phase can be detected in polished alloys as relatively small inclusions which are light after polishing and dark after chemical etching (figure 4.1.1). Usually, the W-phase has no particular shape and has been detected only after the homogenisation of as-melted alloys.[95] A recent article from Gazizov reports that the addition of extra Sc (0.5-0.8 wt.%) leads to the formation of additional amounts of Al_2Cu phase.[96]

There are two main pathways for the formation of W-phase (figure 4.1.2) and they are related to the Al_2Cu-phase (θ-phase). In particular, the W-phase nucleation mechanism is supposed to involve either (i) its growth on an existing θ-phase particle or (ii) the transformation of the θ-phase into the W-phase (due to the diffusion of scandium in the θ-phase from the Al matrix). In the first case, the W-phase constituents must already be in the Al matrix in order to form a nucleus at the interface between the Al matrix and θ-phase. The low interfacial energy associated with this interface would make it a preferred nucleation site. In order for the W-phase to grow, Sc and Cu would diffuse from the θ-phase, thereby consuming it. The W-phase/θ-phase interface would remain unchanged until the θ-phase had been completely dissolved.
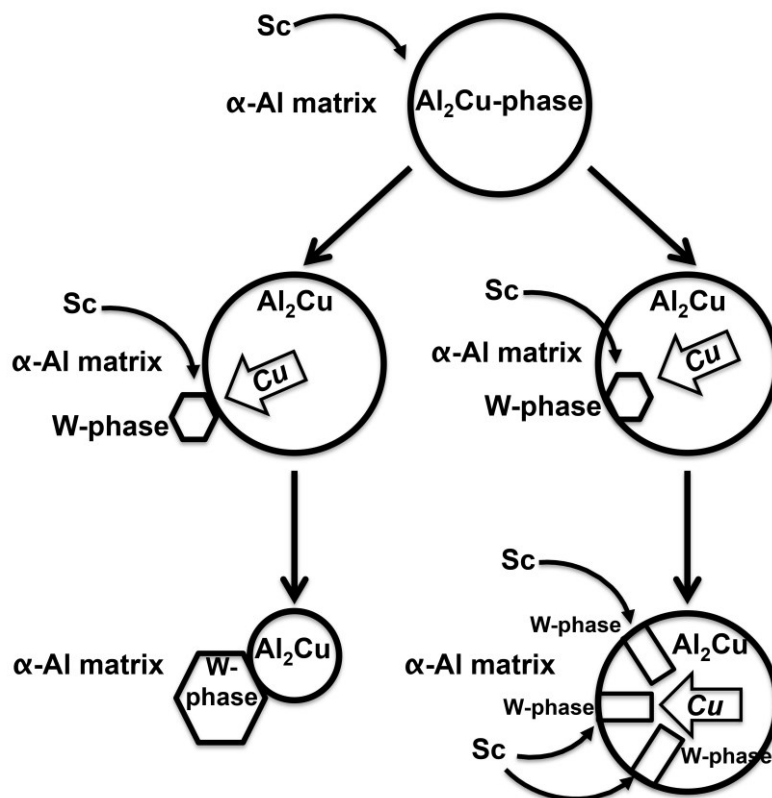
Figure 4.1.2. Formation of the W-phase by nucleation on the Al_2Cu phase (a) and by transformation from θ-phase to the W-phase (b).[96]

Thermodynamic analysis and phase diagrams also suggest a close relationship between Al-Cu phases and W-phase.[97,98] Nevertheless, only a detailed structural analysis of the W-phase would enable us to (i) clarify phase relationships in the Al–Cu–Sc system and (ii) answer the question of how to prevent or take advantage of the formation of W-phase in Al–Cu–Sc multicomponent alloys.

4.2 Al–Co–Sc and Al–Ni–Sc

Bulk-metal glasses based on transition metals have gained importance for their combination of excellent mechanical properties and low cost. Rare-earth based BMGs, on the other hand, are considered promising functional materials. Pioneering studies have been performed on RE–Co and RE–Ni alloys quenched into metallic glassy ribbons and their magnetic properties have been investigated in detail.

Following the discovery that Al and Y additions greatly improved manufacturability and glass-forming ability, a series of Al–Co–Sc bulk-metallic glasses was developed: they exhibit moderate thermal stability and high elastic modulus.[99]

The Al–Co–Sc ternary system has been investigated by Kharakterova et al. Three ternary compounds were discovered.[100] AlCoSc, of $MgZn_{12}$-type hexagonal crystal, has an extended homogeneity range (33-45 at.% Al and 28-37 at.% Sc). A second compound, $Al_{15}Co_8Sc_6$, has $Mn_{23}Th_6$-type cubic structure. Finally, $Al_9Co_3Sc_2$ has the $Ga_9Co_3Y_2$-type orthorhombic structure (*Cmcm*).[101]

Compared with Sc, the solubility of Ni in Al is very limited. Under equilibrium conditions only up to 0.023 at.% Ni is soluble in Al at room temperature. Further addition of Ni leads to the formation of a eutectic between α-Al and the Al_3Ni intermetallic.

The Al–Ni–Sc ternary system comprises five ternary compounds: AlNiSc ($MgZn_2$-type structure), Al_2NiSc ($MgCuAl_2$-type), $AlNi_2Sc$ (Cu_2MnAl-type), $Al_6Ni_2Sc_{0.67}$ ($Al_6Ni_2Y_{0.67}$-type) and $Al_{16}Ni_7Sc_6$ (Th_6Mn_{23}-type).[102]

Among those, AlNi$_2$Sc is reported by Nandi et al. on the grain boundaries of Al–Sc 14 at.% alloys. Coarse and fine dispersions of AlNi$_2$Sc and Al$_9$Ni$_2$ improve hardness and tensile properties respectively.[103]

4.3 Al–Sc–Si: the V-phase

Their low density, castability and mechanical properties make Al–Si alloys industrially appealing. Their microstructure is a mixture of α-Al phase, eutectic Si and intermetallic compounds formed from other alloying additions. Due to the importance given to grain size in the framework of casting alloys it is not surprising that scandium, already successfully used as a grain refiner in Al alloys, has been used in Al–Si alloys as well.

In particular, the addition of Si to Al–Sc alloys results in the formation of a eutectic with low melting point. On the other hand, alloying Al–Si alloys with Sc results in the formation of a ternary V-phase with a slightly decreasing solvus temperature. The formation of the ternary AlSc$_2$Si$_2$ phase, known as V-phase, plays an important role in the metallurgy of Al–Sc–Si based alloys. Scandium segregates to form the V-phase, rather than Al$_3$Sc, due to the higher formation enthalpy of the latter.[104] AlSc$_2$Si$_2$ can be detected as grey inclusions which become black after chemical or electrochemical etching. V-phase particles do not usually have a specific shape.
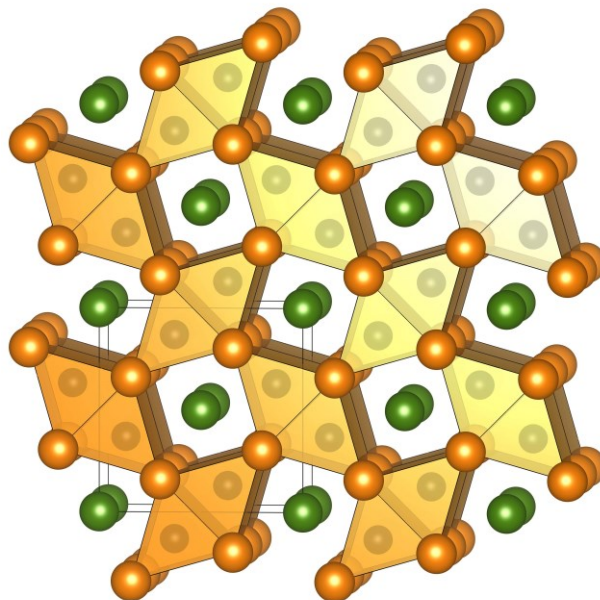
Figure 4.3.1. Crystal structure of AlSc$_2$Si$_2$ compound along the *c*-axis (Al atoms form body-centred cubic packing; connected ScSi$_6$ prisms form chains along the *c*-axis).

According to the recently updated ternary phase diagram, the V-phase shows two invariant reactions:[105]

    (i)   Liq. + Al$_3$Sc = α-Al + V-phase (624.5°C),
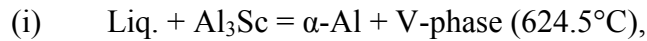
with liquid-phase composition Sc 0.5%, Si 3.5%, Al 96%; and

    (ii)   Liq. = α-Al + Si + V-phase (570.8°C),

with liquid-phase composition Sc 0.2%, Si 8.0%, Al 91.2%.

AlSc$_2$Si$_2$ is the only ternary compound detected in the Al−Sc−Si system and it is in equilibrium with (Si), (Al), Al$_3$Sc and ScSi. AlSc$_2$Si$_2$ has a tetragonal *P4/mbm* space group related to the U$_3$Si$_2$ structural type (figure 4.2.1). The same structure has also been found for the ScNd$_2$Si$_2$ compound, where Sc plays the Al role and Nd replaces Sc. In the crystal structure Si atoms have 6 neighbouring Sc atoms that form an ideal trigonal prism with Sc-Si distances of 2.675 Å. Pairs of trigonal prisms form columns along the *c*-axis with an organisation of hexagonal channels filled with Al atoms. The ternary compound seems to be quite stable with a narrow stability region.[106,107]

4.4. Al−Be−Sc

Chemically stable beryllium containing alloys, often combined with copper, have been proposed for applications in the aerospace industry.[1] The substitution of copper with scandium would further decrease the alloy density, but beryllium toxicity seriously limits the application of its alloys. Nevertheless, the Al−Be−Sc ternary phase diagram has been investigated first by Fridlyander and later by Raghavan.[108,109]

Only binary compounds are formed from the liquid phase. A ternary eutectic (1280(10) °C, 0.1-0.15 at.% Sc) has been detected close to the beryllium rich side. The crystallisation of phases in the ternary system depends on the behaviour of Al$_3$Sc and ScBe$_{13}$ compounds. These should be taken into account in order to further investigate the effect of Be and Sc additions for new and existing multicomponent alloys.

4.5. Sc−Ni−Ti, Rh−Sc−Ti and Rh−Ru−Sc

The Sc-Ni-Ti ternary system has been investigated by Semenova and Velikanova using PXRD, EPMA and DSC.[110-112]

It has been reported that the ternary system can be triangulated along the quasi-binary section TiNi − Sc$_{0.53}$Ni$_{0.47}$ section into two independent subsystems (TiNi − Ni − Sc$_{0.53}$Ni$_{0.47}$ and Ti − TiNi − Sc$_{0.53}$Ni$_{0.47}$ − Sc). No ternary compounds were detected.

The ternary Rh-Ru-Sc system has been investigated in detail by Kornienko and co-authors using PXRD, EMPA and DSC techniques.[113] No ternary compounds were found. The system can be considered as a representative example of a Sc-alloy system with refractory metals. Unfortunately, refractory systems were investigated only in terms of their phase constitution and only sporadic investigations of mechanical and chemical properties were performed. The phase diagram of the Rh–Sc–Ti ternary system has been published by Semenova and co-authors.[114]

The ternary system can be triangulated into two independent sub-systems. Moreover, the RhSc–RhTi section can be considered as quasi-binary. The RhTi and RhSc binary compounds form an infinite series of solid solutions with CsCl structure. It is worth noting that the replacement of titanium by scandium in the RhTi decreases the temperature of the transformations CsCl →AuCu→TiNi and stabilizes the high-temperature phase at room temperature (~30 at.% Sc). Based on the reported decrease of martensitic transformation temperatures, Rh–Sc–Ti alloys were proposed as potential future shape-memory alloys. Recently, the thermo-mechanical and mechanical properties of the Rh–Ti system with Sc additions have been investigated using electrical resistance, dilatometry and three-point bending techniques up to 850 °C.[115] Sc-containing Rh–Ti alloys exhibit continuity of the deformation process on cooling and shape restoration on heating, which makes them promising as heat-regulating elements from room temperature to 850°C. The latest findings show the high importance ascribed not only to the investigation of phase relations in complex Sc-containing systems but also to their mechanical properties, investigated using a broad set of physical-chemical techniques. The reported preliminary results suggest that materials based on ternaries and multicomponent systems containing Sc, Ti, Ni and refractory metals could open up new frontiers in the field of shape-memory alloys and eventually bio-compatible compositions.

4.6. Sc–B–M, Sc–C–M, and Sc–N–M systems

Ternary Sc nitrides and carbides displaying inverse-perovskite type structures (Sc$_3$NM) have been recently proposed as materials with promising physical-chemical properties, such as giant magneto-resistivity and negligible temperature dependence of resistivity. Some inverse-perovskite compounds such as Ni$_3$MgC have superconducting transitions. The appearance of such properties in these ternary phases has initiated many theoretical and experimental investigations in the field of ternary Sc carbides and nitrides.

The crystallographic and stoichiometric features of ternary Sc compounds were discussed in detail in a number of recent reviews.[22,33] It has been reported that the majority of Sc ternary compounds have $ScMX$, $ScMX_2$, ScM_2X and ScM_2X_2 (M – metal, X – non-metal) compositions. It would seem that Sc_3XM stoichiometry is quite rare and appears only in a limited number of ternary systems, mainly in the Sc_3MB (M = Tl, In), Sc_3MC (M = Al, Ga, In, Tl) and Sc_3MN (M = Al, In) systems.[116-118]

Among the ternary compounds of the Sc_3MC_4 (M = Fe, Co, Ni) structure, only Sc_3CoC_4 shows a low temperature phase transition at 72 K with quasi-1D [CoC_4] ribbons responsible for superconductivity below 4.5 K.[119,120]

Extensive experimental investigations on the synthesis and crystal structures of Sc ternaries provide a long list of structural type candidates for further properties investigation. At the same time, experimental data on physical (electrical, magnetic and mechanical) properties is still limited and should be the subject of further studies in the near future. Finally, ternary Sc borides show a large variety of structural types and compositions, especially in the B–C–Sc ternary system.[121] Sc ternary borides with d-block metals display extreme hardness and can be used for the development of wear-resistant alloys.

5.   Scandium Effect

The term 'Scandium Effect' was introduced by Milman et al. in 2000, to indicate the positive influence of scandium additions to the chemical and mechanical properties of aluminium alloys.[122] In particular, this effect was attributed to the formation of the Al_3Sc phase, extremely dispersed and coherently bound with the matrix, heavily influenced by other alloying elements contained in the Al matrix. Milman divided these alloying elements into five classes depending on their physico-chemical interactions with Al and Sc:[123]

- Elements which do not significantly influence the solidus temperature of the alloy, and do not form stable intermetallic compounds with Sc (Ti, Zr, Hf, V, Nb, Ta, Mn, Cr, Mo, W, Re);
- Elements which lower the solidus temperature of the alloy, but are highly soluble in it at 300°C (Zn, Mg, Li);
- Elements which form stable intermetallics with Sc, removing it from the hardening process (Fe, Co, Ni *in primis*, Cu and Si at high concentrations);
- Elements which partially substitute Sc in the Al_3Sc compound, lowering Sc consumption and therefore preserving the hardening effect (Zr, Y).

Using the example of Sc and Zr additions to aluminium alloys, Clouet et al. demonstrated that the effect of adding distinct impurities to a metal does not equate to the summed effect of each of them.[124] However, to a first approximation Milman's classification is consistent with Sc–*M* phase diagrams and with Sc binary formation enthalpies, as well as taking into account the formation of stable ternary intermetallics such as the *V-* and *W- phases* (see sections 2, 3 and 4).

The aim of our review is to extend the concept of the 'Scandium Effect' by highlighting the benefits brought to mechanical properties by the addition of scandium to a variety of multicomponent alloys.

5.1 Addition of Sc to Al

A considerable part of the literature relevant for scandium in aluminium alloys was reviewed by Røyset and Ryum in 2005.[125]

In particular, they have covered the precipitation pathways of Al_3Sc, the compound responsible for the improved mechanical features of the Al-based alloys, as well as the macroscopic influence of scandium on microstructure and properties (grain refinement, strengthening effect and corrosion resistance).

While the amount of information on several Al-containing systems has increased considerably in the last ten years, subsequent papers have mostly confirmed Røyset assessment. Only a few of the Al-based systems studied have undergone significant further development and these are reviewed here. In particular, the effect of scandium additions to Al−Si and to Al−Ti alloys will be discussed.

5.1.1 Addition of Sc to Al−Si, Al−Fe−Si and Al−Mg−Si alloys

The high specific strength, stiffness, hardness and resistance to wear and elevated temperature make Al-matrix composites and Al−Si alloys extremely attractive for industrial applications. Al−Si alloys, in particular, offer outstanding casting properties, which can be tuned with proper treatments. A critical role in casting is played by the dimension and morphology of primary and eutectic silicon. Modification of silicon particles can be achieved with different techniques, such as spray forming, centrifugal casting, high current electron beam, gas atomization, spark plasma sintering, melt-spinning, *etc*. However, melt treatment combined with the addition of chemical modifiers (e.g. Na, K, Sr and Ca) is regarded as the most effective and simplest method.

The eutectic Si in Al−Si alloys (see section 2) grows in a facetted way according to the Twin Plane Re-entrant Angle Edge (TPRE) mechanism. The Si phase grows parallel to the existing Si twin plane forming coarse angular plates and needles which reduce the mechanical properties of the alloy.[126]

However, when modifiers are added to the melt they can be absorbed onto the surface of the eutectic Si and change its growth mode from TPRE to IIT (Impurity-Induced Twinning).[127] As a consequence, the morphology of the eutectic silicon changes to very fine, branched plates with rounded edges. In fact, atoms of the modifier are absorbed at the growth steps of the Si solid-liquid interface. If the ratio between the atomic radius of the modifier and silicon is close to 1.65 a growth twin will occur at the interface. As modifiers concentrate in the Si phase instead of the Al phase the eutectic growth mechanism changes from TPRE to IIT. Modifiers also decrease the surface tension of Al−Si alloys. As a consequence, the contact angle between the Al and the Si phase increases, Al can easily wet the Si phase and the growth of facetted eutectic silicon is restricted.

The well-known positive effects of scandium additions to aluminium alloys made it a promising candidate to act as chemical modifier in Al−Si hypereutectic alloys. However, as pointed out by Pramod *et al*., Sc has an atomic radius ratio with Si of 1.4, definitely lower

than the 1.65 required by the IIT mechanism. As a consequence, Sc does not segregate to the eutectic Si phase, but dissolves in (Al) and in the $AlSi_2Sc_2$ V-phase.[128]

However, Kim *et al.* pointed out that the addition of scandium to Al−8.5 wt.% Si alloys modifies the silicon eutectic by reducing the surface tension of the melt.[129]

Prukkanon *et al.* performed small (0.2 and 0.4 wt.%) additions of Sc to the hypoeutectic Al−6 wt.% Si−0.25 wt.% Mg alloy and reported a change in eutectic morphology towards a fine fibrous structure, as well as a reduction in eutectic temperature (from 573.4 to 566.7°C) and an increase in recalescence (from 0.68 to 3.39°C when 0.2 wt.% Sc was added and to 5.04°C when 0.4 wt.% Sc was added). The lowering of the eutectic growth temperature is directly related to the modification of the Si morphology, whereas an increase in recalescence is an indication of a nucleation effect due to the absorption of impurity elements on the interface between Si and liquid Al.[126]

Prukkanon *et al.* carried out fluidity tests on A356 alloys modified with 0.2 wt.% Sc, 0.4 wt.% Sc and 0.2 wt.% Sc+0.2 wt.% Zr and found that Sc-modified samples displayed a 40% increase in fluidity due to effective grain refinement.[130] Patalham *et al.* also performed tests on A356 alloy and noticed a low grain refining effect due to Sc additions, which was attributed to heterogeneous nucleation.[131] Zhang *et al.* found significant changes in the microstructure (figure 5.1.1) of Al-7wt.% Si alloys when the Sc content was increased to 0.15%. In particular, Sc was found in the interdendritic region and in a fish-bone structure consisting of $AlSc_2Si_2$ V-phase and iron.[132]
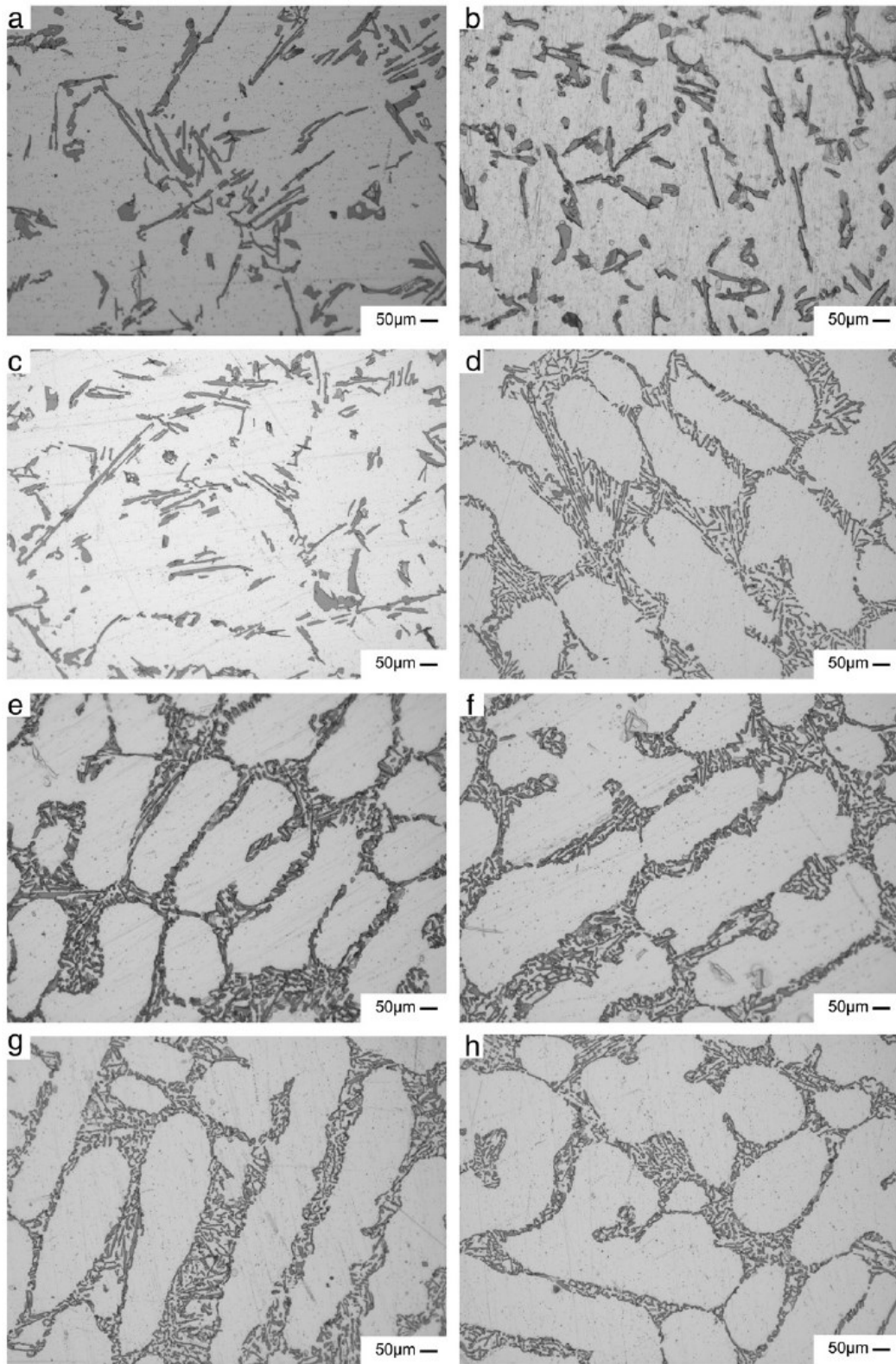
Figure 5.1.1. Dendritic microstructures of as-cast alloys with increasing Sc content. a) Al–7 Si alloy with no Sc. b) +0.05 wt.% Sc. c) +0.10 wt.% Sc. d) +0.15 wt.% Sc. e) +0.20 wt.% Sc. f) +0.25 wt.% Sc. g) +0.30 wt.% Sc. h) +0.40 wt.% Sc.[132]

Rajinikanth *et al.* processed Al–2 wt.% Si–0.25 wt.% Sc by high-pressure torsion and measured a grain size 40 % smaller than that obtained for Al–2 wt.% Si under the same conditions.[133] The formation of an Fe-modified V-phase and the grain refining reported by Prukkanon and Zhang has been recently confirmed by Pramod *et al.*[128] With respect to common A356 alloy modifiers (Al–B–Ti and Sr), which influence only one microstructural feature, the addition of Sc to Al–Si alloys causes both eutectic Si modification and grain refinement at the same time.

Sc addition has a positive influence on hardness and tensile strength (figure 5.1.2). Moreover, Pramod *et al.* reported an increase in hardness of 20 % for a 0.4 wt.% Sc addition to A356 alloy.[128]
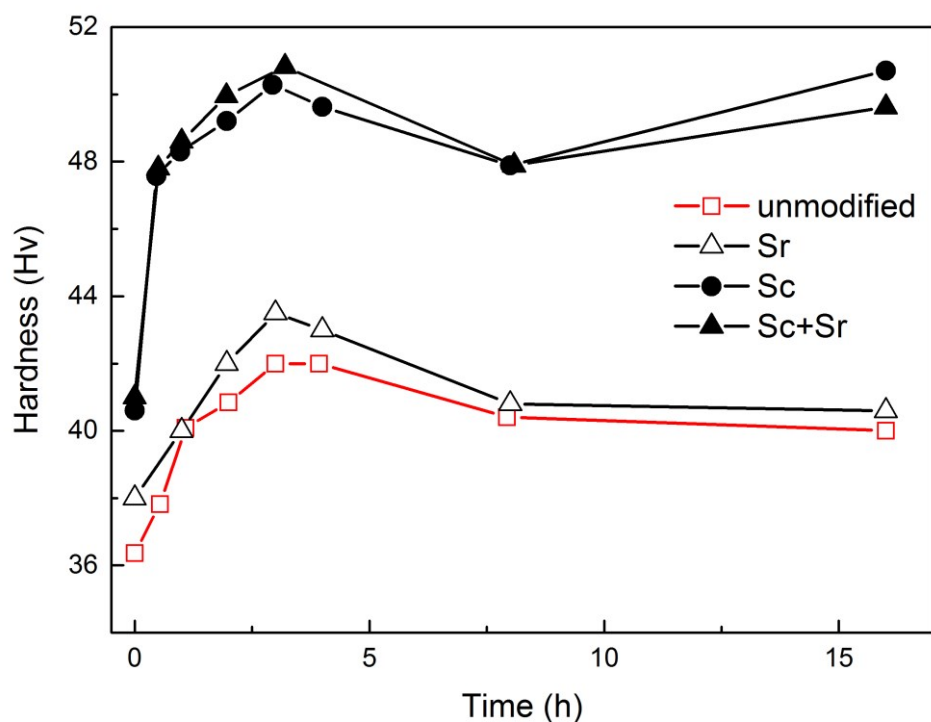
Figure 5.1.2. Vicker's hardness of Al-8.5 wt.% Si alloys with various modifiers according to heat-treatment conditions (200°C for 0~16h).[134]

Kim *et al.* studied the change in mechanical properties after increasing additions of Sc to the Al–8.5 wt.% Si alloy: they reported a 60 % increase in tensile strength, a 50 % increase in elongation and observed that hardness increased until the Sc content reaches 0.8 wt.% subsequently decreasing up to a 1.6 wt.% Sc addition. The optimum amount of 0.8 wt.% Sc

corresponds to the finest Si eutectic morphology (higher Sc additions corresponded to Si eutectic over-modification).[134]

5.2 Addition of Sc to Al−Ti alloys and to Mg−Mn alloys
5.2.1 Cast Alloys

For Ti, Al and Mg-based casting alloys the addition of RE elements has been shown to be beneficial although the use of Sc as the RE element is not yet fully explored. In aluminium alloys the effects of small Sc additions are threefold.[135] Firstly, scandium acts to raise the recrystallization temperature thus reducing the tendency to recrystallization with the formation of a fine dispersion of Al_3Sc (L12) particles.[135-137] These particles are coherent with the matrix and as long as a small interparticle distance is maintained the reduced tendency to recrystallization persists. However, a loss of coherency leads to rapid growth and coarsening of Al_3Sc particles leading to the disappearance of the anti-recrystallization effect. The addition of small (0.1%) amounts of Zr can improve the situation with the formation of $Al_3(Sc_{1-x}Zr_x)$ particles which are less susceptible to coarsening. Small additions of Ti to an Al−Sc alloy also retarded the coarsening kinetics of precipitates via the formation of $Al_3(Sc_{0.94}Ti_{0.06})$ particles although not as effectively as Zr additions.[138] Secondly, the presence of a fine dispersion of Al_3Sc particles provides a significant precipitation strengthening effect. Post-solidification homogenization techniques are often used to ensure unwanted phases formed by major alloying elements are dissolved and a fine dispersion of Al_3Sc particles can form from a supersaturated solution of Sc (and Zr). Lastly, during casting of Al alloys the Al_3Sc particles forming in the liquid provide a high density of nucleation sites for solidification of equiaxed grains giving rise to a Hall-Petch type of strengthening.

In Al containing Mg-based casting alloys additions of rare earth (RE) elements such as La, Pr and Ce have been shown to produce excellent grain refinement.[139] For cast Al−Mg alloys additions of small amounts of RE have been shown to provide improved properties e.g. for alloys AZ91−x RE and Mg−6 wt.% Al−x RE casting fluidity and as-cast hardness increased as did high temperature tensile properties.[140] The sand cast and heat-treatable (T6) AM-SC1 Mg-alloy (1.7 wt.% Nd, 1.0 wt.% RE, 0.5 wt.% Zn plus Zr for grain refinement) displays excellent creep resistance at the elevated temperatures required for modern engine blocks partly attributable to the formation of intergranular $Mg_{12}RE$ phase (see section 3).[141] The creep resistance of RE-containing Mg-alloys is usually exploited in aerospace applications

due to the high costs associated with RE elements (typical alloys include AE42, EZ33, WE43, WE54, ZE41 and ZE63).[139] For pressure die-cast commercially pure Mg, additions of up to 5 wt.% of La, Ce and Nd led to improved yield strength and ductility attributed to intermetallic phases $Mg_{12}La$, $Mg_{12}Ce$ and Mg_3Nd forming in the eutectic.[142] A series of cast MgLiAlZn–x RE alloys (where RE = La, Pr and Ce) also exhibited improved high temperature strength attributed to the formation of rod-shaped Al_2Zn_2La intermetallic phase distributed in the matrix.[143]

For cast alloys based on Ti the picture is similar. Minor additions of Sc (up to 0.4 at.%) to Ti–Al based alloys (Ti– 43 wt.% Al and Ti– 48 wt.% Al) produced increased high temperature compressive strengths with the formation of $Ti_3(Al,Sc)$ plate precipitates mainly along α_2/γ or γ/γ_T boundaries providing an obstacle to interlamellar sliding and dislocation movement.[144] For binary Ti–x Sc alloys with much larger additions ($x = 2, 5, 25$ and 37) the addition of Sc acted as a grain refiner with an associated increase in hardness but also as a β-stabiliser, producing very different microstructural morphologies.[145] β-stabilisers in cast Ti–Al alloys have been shown to improve ductility.[146] The Al–Nb–Ti system has also been investigated where cast and homogenized Ti– 40 wt.% Al –16 wt.% Nb with additions of 0.39 wt.% M (M = Sc or La-rich Misch metal) were studied.[147,148] However, in this case homogenization temperatures of 1100ºC (albeit under a positive pressure of Ar) led to the formation of a fine dispersion of cubic Sc_2O_3 (or spheroidal La_2O_3) oxide particles via internal oxidation. Again, the small RE additions alter the phase transformations occurring by possibly stabilising and extending the disordered α_2 phase while decreasing the amount of γ phase. In this case superior high temperature mechanical properties can be attributed to the fine oxide dispersion acting as a barrier to dislocation movement. For a series of directionally solidified Ti– 45 wt.% Al– 3 wt.% Nb (Cr,Mn,Mo,Sc) alloys minor Sc additions coupled with complex microalloying of Cr, Mn and Mo led to improved high temperature mechanical properties arising from a refinement of interlamellar spacings and the dispersive strengthening effect of $Ti_3(Al,Sc)$ dispersoids.[149] Additions of Cr and Mo alone provide improved high temperature creep properties.[150]

5.2.2 Wrought alloys

For wrought materials the commonly used Ti– 6 wt.% Al– 4 wt.% V alloy (cast, homogenized and forged) has been studied. Internal oxidation of minor Sc additions forms Sc_2O_3 dispersoids (see section 3) but no clear strengthening effect was observed.[151] The

benefits of Sc additions to wrought Al–Mg alloys have been shown to produce alloys of high strength, good corrosion resistance and excellent electrical and thermal conductivity.[152] Al–Mg–Sc–Zr alloys produced via powder metallurgy and then extrusion showed the strengthening effect of fine $Al_3(Sc,Zr)$ particles.[153] The rolled Al–Mg based alloy 5754, with minor Sc and Zr additions, showed improved mechanical and fatigue properties. In this case two populations of $Al_3(Sc,Zr)$ particles are observed, large incoherent precipitates formed during solidification and hot rolling and fine coherent precipitates formed via secondary precipitation. The fine $Al_3(Sc,Zr)$ particles provide a strengthening effect although these particles are destroyed during annealing and the formation of Al_6Mn and β-Al_3Mg_2 grain boundary precipitates results in poorer fatigue performance and reduced ductility.[154] Extruded and heat treated Al–Zn–Mg–Cu–(Sc,Zr) alloys have been studied to assess the effects of hot-working and post heat treatment. These alloys showed improved properties with minor Sc additions.[155]

5.2.3 Creep properties

Sc additions to improve creep properties have been mainly focussed on Mg– and Ti–Al-based alloys. In Ti–Al alloys additions of Si, N and C have been shown to improve creep resistance.[156-158] Minor additions of Sc to make a Ti–40wt.% Al–16wt.% Nb–0.4wt.% Sc alloy resulted in a fine dispersion of Sc_2O_3 particles and increased creep performance.[159] For Mg-based alloys creep resistance at about 300ºC for automotive applications is of interest. Following preliminary studies of the Mg–Sc–Mn system, Mordike examined squeeze cast Mg–Sc and Mg–Gd binaries, an Mg–Sc–Mn ternary and several quaternaries Mg–Mn–(Sc–Ce, Gd–Sc, Y–Sc).[160,161] For the Mg–Sc binary no precipitation or improvement of creep properties is observed. However, for the Mn containing alloys precipitation of Mn_2Sc (both within grains and at grain boundaries) was observed in the as-cast and T5 heat treated conditions and creep resistance is improved significantly. Zr was not used in this work but the paper highlighted the potential scope to develop new creep resistant Mg alloys. Subsequently the squeeze cast Mg–RE–Sc–Mn (RE = Gd,Y,Ce) system was investigated, where the formation of fine particles of stable Mn_2Sc phase coupled with Mg_5Gd led to improved creep resistance.[162-164] In an attempt to reduce the cost of Sc bearing alloys the replacement of 0.9 wt% Sc with 1.0 wt.% Zn in the Mg–3wt.% Ce–1.2 wt.%Mn–0.9wt.% Sc alloy was investigated.[165] The as-cast microstructure of the Sc containing alloy consisted of α-Mg, $Mg_{12}Ce$ and Mn_2Sc phases whereas the Zn containing

alloy consisted of only α-Mg and $Mg_{12}Ce$ phases. Although the room temperature tensile properties of both alloys were similar, the creep resistance at 300ºC was greater in the Sc containing alloy.

5.2.4 Fatigue properties

Fatigue studies have largely concentrated on wrought Al- or Mg-based alloys. Two wrought Al–5 wt.% Mg–0.3wt.% Mn–0.06wt.% Zr alloys, with and without 0.25wt.% Sc, were assessed and the Sc containing alloy showed higher tensile yield stress, higher fatigue strength values and a higher resistance to microcrack growth, attributed to the presence of coherent $Al_3(Sc,Zr)$ precipitation strengthening and a stabilising effect on subgrain boundaries during processing resulting in a finer grain structure.[166] However, the Sc-free alloy was more resistant to macrocrack growth due to its coarser grain structure. Similarly, an Al–4wt.% Mg–0.3wt.% Sc alloy was found to have generally superior fatigue properties compared to the standard Al-alloy 6013 T6, although once again the Sc-free alloy 6013 was better at resisting macrocrack propagation.[167] When Al–Mg–Sc alloys are produced using severe deformation methods only modest improvements over ordinarily fabricated material are achieved.[168] RE additions to Mg-based alloys are known to improve ductility, refine grain size and weaken recrystallization textures and improve fatigue performance, although additions of RE elements other than Sc are more commonly reported.[169-175]

5.3 Addition of Sc to steel

The addition of scandium to various steel types has been investigated to predict possible improvement of steels mechanical features after Sc-doping.[176-178] Scandium has been added up to 5 wt.% leading to decreased viscosity and surface tension of liquid steel.

In general, Sc addition improves the homogeneity of liquid and solid steel, as well as the mechanical properties of final doped steels. In fact, due to the high affinity of Sc for C, O and N, small Sc additions to steels reduce the concentration of non-metallic elements, which could be one reason for the observed changes in mechanical properties.

The chemical reaction occurring between Sc and non-metals dissolved in steels causes Sc to effectively disappear as an alloying element and reducing its potential activity as a doping component. In this way the high chemical activity of Sc limits its application as an alloying element for steels. The enhanced properties which can be achieved by Sc additions are not

enough to justify its cost. Scandium does not behave as a proper alloying element but rather as a compound-forming element in the proximity of grain boundaries.

5.4 Effect of Scandium small addition to alloys containing an intermetallic-forming element

Original alloy	Effect of Sc addition	Responsible compound
Al	Grain refinement Precipitation hardening Increased superplasticity Recrystallisation resistance Corrosion resistance	Al_3Sc
Al–Ni	Increased hardness Increased tensile properties	$AlNi_2Sc$; Al_9Ni_2
Al–Si	Grain refinement Precipitation hardening Si eutectic modification Increased fluidity Increased tensile strength	$AlSi_2Sc_2$ (V-phase)
Al–Ti	Grain refinement Precipitation hardening Increased ductility Increased compressive strength	$Ti_3(Al,Sc)$; Al_3Sc
Al–Mg	Precipitation hardening Corrosion resistance Increased electrical/thermal conductivity	Al_3Sc
Mg–Mn	Grain refinement Increased creep resistance Increased ductility Increased fatigue resistance	Mn_2Sc
Steel	Increased homogeneity Decreased viscosity Decreased surface tension	Sc_2O_3

Table 5.4: Effect of Sc additions on the properties of multi-component alloys.

The effect of the addition of scandium to multicomponent alloys is strictly dependent on the presence of intermetallic forming elements in the matrix (see section 2).

The formation enthalpy values of scandium binary compounds with non-metals are very low, making their precipitation favoured with respect to metallic binary compounds (see section 3 and Supporting Information). This trend is consistent with the frequent formation of Al_3Sc in aluminium containing alloys and of Sc_2O_3 when non-metal impurities are present in the bulk alloy, as well the formation of the V-phase in Al–Si alloys. Whenever such elements are not present, however, scandium forms intermetallic compounds with metals (Mn_2Sc and possibly Ni_5Sc).[179]

In all cases, the small addition of scandium and the precipitation of binary and ternary intermetallics leads to enhanced mechanical properties (table 5.4), in particular grain refinement and precipitation hardening. Moreover, the high stability of scandium intermetallic compounds makes them resistant to recrystallization. However, while such features can be obtained with the addition of less expensive elements, scandium often improves ductility, viscosity, creep and fatigue resistance and corrosion.

6.   Scandium as alloying element

The high cost and low availability of scandium, as well as the low amount required to bring forth its peculiar mechanical effects, all help to perpetrate the idea of Sc as a 'spice metal'. As such, scandium has always been used as a small addition, for Al alloys first and increasingly now to multicomponent alloys. Far from making scandium more accessible, its limited use for functional alloying makes it a 'consumable', impossible to actively recycle because of the minor concentrations in operation.[180]

On the other hand, the literature describing scandium as a major alloying element is limited, and not older than ten years. Given the surprising properties of Sc alloys, interest in this research field is sure to grow in the future. Scandium alloys have been successfully implemented as hydrogen-storage materials, in High-Entropy Alloys (HEAs) and in bulk metallic glasses. In each case, the alloying has resulted in a new material of lower density and higher hardness.

These recent findings will be reviewed in the next sections.

6.1 80wt.% Mg –20wt.% Sc as hydrogen storage material

Hydrogen can easily be produced during electrochemical water-splitting. Its low weight makes it suitable for portable applications and it is disposable with clean reactions. However, the storage of such a highly reacting gas remains a serious problem. The challenge is to find a way to store large quantities of hydrogen in a small volume. While high-pressure compression and liquefaction present dangers and require elevated temperatures, the use of hydrogen-storage materials, able to operate at moderate temperature and pressure values, remains a challenge.

One of the most popular classes of hydrogen-storage materials is metal hydrides. These are crystals which can host hydrogen atoms in their vacancies and release them with a doping-undoping reversible process. From these materials MgH_2 shows a high reversible storage capacity (7.6 wt.% hydrogen). However, its slow absorption kinetics and high operating temperature make it uncompetitive. To enhance the properties of Mg hydrides researchers have tried to reduce Mg particle size, alloy Mg with other metals or adsorb catalyst particles onto the Mg surface.[181] Alloying with other metals might enable one to maintain the high storage capacity of Mg while combining it with the superior kinetic diffusion rates typical of metal hydrides. Recent studies confirmed that Mg−RE alloys with a high Mg content could store large amounts of hydrogen while retaining RE fast absorption kinetics. In particular,

when Mg (up to 80%) was alloyed with Sc, the alloy displayed high reversible storage capacity (6.7 wt.% hydrogen) and very good rate capabilities.

Further studies revealed that catalysts such as Pd or Rh were crucial in enhancing the hydrogen absorption of the alloy. This led to understanding that in order to produce competitive materials the hydride fluorite structure was decisive. The expansion of the fluorite lattice is believed to allow hydrogen to partially occupy its octahedral interstitial sites.[182,183]

Finally, both bulk and thin film electrodes were produced and tested.[184] Recent advances in Mg alloy hydrides have been extensively reviewed by Manivasagam et al.[185]

6.2 Biodegradeble Mg–Sc and Mg–Y–Sc alloys

Recently, Mg–Sc and Mg–Y–Sc alloys (Mg–wt.% 3wt.% Sc and Mg–3wt.% Sc–3wt.% Y) were proposed as biodegradable alloys. Brar et al. reported that the alloying of Mg with rare-earth metals and Sc significantly influences oxidation rates with the formation of a self-passivating oxide layer.[186,187] Compared with a polished surface, the oxide layer reduces degradation rates by almost a hundred-fold (to 0.01 ml cm^{-2} day^{-1} for up to 23 days). Nevertheless, practical use of such materials is not expected due to their high toxicity to osteoblastic cells.

6.3 New Sc-containing high-entropy alloys and Sc-based metallic glasses

High-entropy multicomponent alloys (HEAs) and bulk metallic glasses (BMGs) have been proposed as potential future functional materials.[188] Introducing Sc into existing alloys and the development of new compositions may result in improved mechanical and chemical properties, as well as lower density – a decisive feature for future applications. Until now only pilot experimental work has been performed with Sc-based HEA and BMG alloys. Nevertheless, their output is quite promising. Following pioneering works, where Co–Sc and Fe–Sc BMG with modest characteristics were prepared, several Al–Co–Y–Sc BMGs were synthesized.[189-193] The resulting Sc-based BMGs exhibit outstanding values of elastic moduli (e.g. Young's modulus, E = 85 GPa; bulk modulus, B = 77.5 GPa), glass transition temperature (T$_g$ = 662 K), and crystallization temperature (T$_x$ = 760 K) combined with a large region of supercooled liquid (dT = 98 K).

In the framework of HEAs, Al was selected as a main alloying element due to its tendency to encourage crystallization towards the *bcc* crystal structure. The well-known improved mechanical properties related to the addition of Sc to common Al alloys made it an obvious

candidate for Al-containing HEA. Nevertheless, it was only in 2014 that the first Sc-based HEA was described in the literature.[194]

Rational prediction of the composition for single-phase low-density HEAs resulted in the preparation of $Al_{20}Li_{20}Mg_{10}Sc_{20}Ti_{30}$ using cryogenic ball-milling, followed by further milling at room temperature. The as-synthesized material has an *fcc* structure which changes to *hcp* after homogenisation at 500 °C. The resulting alloy has extremely low density (2.67 g cm^{-3}) combined with a high hardness. Moreover, its estimated strength-to-weight ratio is significantly higher than other nanocrystalline alloys, almost comparable with ceramic materials.

Following the success of these experiments, pilot studies were performed in order to obtain multi-component alloys containing high concentration of scandium via direct melting.[195]

7. Conclusion and future perspectives

The body of published investigations provides a deep insight into scandium-based thermodynamic and phase equilibria, building a bridge between simple phase diagrams, phase stability and functional properties. Raising awareness of the importance of scandium as a major and minor addition element in the framework of alloy design provides a foundation for the development of new multicomponent alloys with competitive mechanical properties. Knowledge of scandium alloys and intermetallic compounds has been reviewed and critically analysed, starting from the well-studied forefather system (Al−Sc) and moving to less common but equally functional alloys (*inter alia* Mg−Mn, Ti−Al, steel). Data from international databases, phase diagrams and individual publications have been collected and errors and inconsistences have been highlighted.

Elemental scandium displays a rich high-pressure phase diagram with the formation of five unique high-pressure modifications at room temperature. The incommensurate Sc-II polymorph shows a superconducting transition below 19.7 K at 107 GPa. The superconductive temperature of Sc−II is the second highest observed for pure elements investigated under pressure. Despite this, the superconducting properties of scandium intermetallics are largely unexplored. The presence of pressure-induced superconductivity in scandium-based intermetallic compounds and alloys warrants much more experimental investigation. In fact, the sporadic investigation of pressure-induced transformations in Sc−Zn and Sc−Ga binary systems highlights complex high-pressure high-temperature phase relations which can be related to the Sc electron configuration ($4s^2 3d^1$). Further detailed investigation of binary and ternary systems will enhance our understanding of the general trends of transformations induced by high-pressure and high-temperature. Undoubtedly, several unusual Sc binary and ternary phases with promising functional properties will be found in the near future.

Detailed crystallographic analysis of existing Sc binary and ternary compounds makes it possible to identify trends in their appearance, crystallographic structure and stability. Formation enthalpy values explain the easy precipitation of Al_3Sc in Al−Sc alloys and highlight the existence of potential alternative compounds which may give equally controlled dispersion. The effect of such intermetallics on the properties of selected alloys (*i.e.* Al─Sc─Si and Al─Cu─Sc) has been reviewed. The presence of analogous compounds in other barely-investigated systems (*e.g.* Al−Ni−Sc, Al−C−-Sc as compared to Al−Cu−Sc) may enable us to predict similarities in their properties and eventually improve the functional

properties of known alloys. As another example, the implementation of magnetically active Ni and Co could induce magnetic activity still unknown for existing multicomponent systems.

The precipitation of scandium compounds has been related to an improvement in mechanical properties. The examples described here show that the precipitation of intermetallics (Al_3Sc, Mn_2Sc) of low formation enthalpy in equilibrium with the Al− and Mn−rich phases leads to grain refinement, higher creep resistance, increased hardness and improved tensile strength. It is also apparent that in the absence of intermetallic-forming elements scandium easily oxidizes to form Sc_2O_3, the only advantage of which is an increase in hardness due to dispersion hardening.

The use of scandium is limited by its high prices and low availability in the market. Previously, the progress in Sc metallurgy has been driven by its relatively large production in the Soviet Union and its rareness in other countries. As such, the most widespread use of Sc was for aircraft and space programs based in the Soviet Union and modern Russia. However, recent progress in the use of Sc in manufacturing, combined with the appearance of new mining projects with ambitious production plans, will make large quantities of Sc available on the market and eventually stimulate detailed investigation of its multicomponent alloys. In this framework, the investigation of compound-forming systems such as Al−Cu−Sc, Al−Sc−Si and others can prove to be the key for a drastic improvement in manufacturing and casting routes.

With its price decreasing, eventually scandium will not only be considered a 'spice metal' (a term coined to describe its major effect when added in small quantities to Al-based alloys), but also as an active alloying element, a major component of a novel generation of complex functional alloys. On this point, the investigations of $Mg_{80}Sc_{20}$ and $Al_{20}Li_{20}Mg_{10}Sc_{20}Ti_{30}$ highlight how scandium can contribute to the development of novel HEAs.

To speed up the development of new scandium-based multicomponent alloys, modern material screening techniques will be required. In fact, models have been used recently to predict the appearance of Sc intermetallic compounds in multicomponent alloys, ($AlSc_3$ in Al−Sc−Zr), and the stability at moderate and high temperatures of new compositions (AFLOW computational database).[31,196]

High-throughput screening using spattered thin films as well as diffusion multiples will increase the success rate of alloy development and strengthen our understanding of the link

between structure and properties. Such approaches can only accelerate discovery of new materials in this largely unmapped space.

Acknowledgments

LIST OF FIGURE AND TABLES CAPTIONS

Figure 1.2.1. Crystal structure of room temperature *hcp* α (Sc) along *c*-axis (*left*) and high-temperature *bcc* β (Sc) (*right*).[5]

Figure 1.2.2. Crystal structure of high-pressure tetragonal incommensurate Sc-II phase along *c*-axis. The figure shows two crystallographically independent Sc atoms forming host framework (*yellow*) and guest atoms (*green*).[5]

Figure 1.2.3. Crystal structure of high-pressure hexagonal Sc-V phase along *a*-axis (*left*) and *c*-axis (*right*).[5]

Figure 3.4. Scandium and Sc_2O_3 (99.99% purity) price in US$/g. Courtesy of U.S. Geological Survey, Mineral Commodity Summaries, years 2003-2014.

Figure 4.1 Scandium phase diagrams State of the Art. In red are phase diagrams studied over the whole composition range; in blue are binary phase diagrams covered only partially; in green are systems where information comes only from ternary phase diagrams; in white are currently unknown phase diagrams.

Figure 2.1.1. Sc–Hf phase diagram.[23]

Figure 2.1.2. Sc–Li phase diagram.[24]

Figure 2.1.3.1. Sc–Cr (*left*) and Sc–V (*right*) binary phase diagrams.[24,25]

Figure 2.1.3.2. Sc–Ce binary phase diagram.[26]

Figure 2.1.4. Sc–Pd binary phase diagram.[27]

Figure 2.1.5. Sc–Tl binary phase diagram.[28]

Table 2.2.1. Problematic phase diagrams of binary systems.

Figure 3.1. Overview of scandium binary intermetallics according to literature search and a 1998 paper from Kotur.[33]

Figure 3.2.1. Polyhedra for $ScIr_6$ (in the crystal structure of $IrSc_2$), $ScSn_7$ (in the crystal structure of Sc_5Sn_3), $ScIr_{12}$ (in the crystal structure of Sc_2Ir), $RhSc_7$ (in the crystal structure of $Sc_{57}Rh_{13}$), and $IrSc_8$ (in the crystal structure of $Sc_{44}Ir_7$).

Figure 3.2.2. $ScSn_2$ crystal structure (*I4/amd* space group) along *a*-axis (orange spheres represent Sc and green spheres represent Sn).

Figure 3.2.3. Polyhedral representation of crystal structures of the Au_2Sc crystal structure along the *a*-axis (*I4/mmm* space group, *left*) and Au_4Sc along the *c*-axis (*I4/m* space group, *right*) (Sc polyhedra are shown).

Figure 3.2.4. Fragment of Ir_4Sc_{11} crystal stracture (*left*) showing interconnected $IrSc_4$ planar squares (*Fm$\bar{3}$m* space group) and the complete structure (*right*) along the *c*-axis.

Figure 3.2.5. α-, β- and γ-Fe_2Se along the *c*-axis (green spheres represent Fe atoms, orange spheres represent Sc).

Figure 3.2.6. Ni_5Sc crystal structure (*P6/mmm* space group).

Figure 3.4.1. Ambient-pressure along *b*-axis (*left*) and high-pressure (*right*) phases of $ScGa_2$.

Figure 3.4.2. $ScZn_{12}$ coordination polyhedron (*left*) and high-pressure crystal structure of $ScZn_2$ (*right*).

Figure 4.1.1. Representative structure of Ag–Al–Cu–Mg alloy with Sc addition observed by bright-field TEM.[94]

Figure 4.1.2. Formation of the W-phase by nucleation on the Al_2Cu phase (a) and by transformation from θ-phase to the W-phase (b).[96]

Figure 4.3.1. Crystal structure of $AlSc_2Si_2$ compound along the *c*-axis (Al atoms form body-centred cubic packing; connected $ScSi_6$ prisms form chains along the *c*-axis).

Figure 5.1.1. Dendritic microstructures of as-cast alloys with increasing Sc content. a) Al–7 Si alloy with no Sc. b) +0.05 wt.% Sc. c) +0.10 wt.% Sc. d) +0.15 wt.% Sc. e) +0.20 wt.% Sc. f) +0.25 wt.% Sc. g) +0.30 wt.% Sc. h) +0.40 wt.% Sc.[132]

Figure 5.1.2. Vicker's hardness of Al-8.5 wt.% Si alloys with various modifiers according to heat-treatment conditions (200°C for 0~16h).[134]

Table 5.4: Effect of Sc additions on the properties of multi-component alloys.

REFERENCES

1. J.C. Williams and E.A. Starke, Jr.: 'Progress in structural materials for aerospace systems', *Acta Mater.*, 2003, **51**, 5775-5799.

2. I.N. Fridlyander: 'Modern aluminium and magnesium alloys and composite materials based on them', *Met. Sci. Heat Treat.*, 2002, **44** (7-8), 292-296.

3. FTAP First Cycle, Final Report 2012.

4. D. Hunn: 'Lockheed Martin armor developments ', *Adv. Mat. Processes*, 2006, **164** (10), 23.

5. D.R. Kammler, M.A. Rodriguez, R.G. Tissot, D.W. Brown, B. Clausen and T.A. Sisneros: 'In-situ time-of-flight neutron diffraction study of high-temperature a-to-b-phase transition in elemental scandium', *Met. Mater. Trans. A*, 2008, **39** (12), 2815-2819.

6. M. Debessai, J.J. Hamlin and J.S. Schilling: 'Comparison of the pressure dependences of T_c in the trivalent d-electron superconductors Sc, Y, La, and Lu up to megabar pressures', *Phys. Rev. B*, 2008, **78**.

7. C. Buzea and K. Robbie: 'Assembling the puzzle of superconducting elements: A Review.' *Supercond. Sci. Technol.*, 2005, **18.**

8. S.A. Wood and I.M. Samson: 'The aqueous geochemistry of gallium, germanium, indium and scandium', *Ore Geology Rev.*, 2006, **28**, 57–102.

9. W. Wang, Y. Pranolo and C.Y. Cheng: 'Metallurgical processes for Scandium recovery from various resources: A review.' *Hydrometall.*, 2011, **108**, 100-108.

10. William T. Tack, Arhurst Technology Corporation: 'Aluminium-scandium alloys', US Patent 5597529, published 28 January 1997.

11. J.A. Lee and P.S. Chen: 'Aluminium-Scandium alloys: Material characterization, friction stir welding, and compatibility with hydrogen peroxide', MSFC Center Director's Discretionary Fund Final Report, Project No. 04-13, Marshall Space Flight Center, Alabama, USA, 2004.

12. T. Wohlers and T. Caffrey: 'Additive manufacturing : going mainstream', *Manuf. Eng.*, 2013, **5**.

13. W.E. Frazier: 'Metal additive manufacturing: A review', *J. Mater. Eng. Perform.*, 2014, **23**, (6), 1917–1928.

14. T. Wohlers and T. Gornet, 'History of additive manufacturing,' Wohlers Report 2012, Wohlers Associates Inc., 2012.

15. J. Røyset: 'Scandium in Aluminium alloys overview: Physical Metallurgy, Properties and applications', *Metall. Sci. and Technol.*, 2007, **25** (2), 11–21.

16. K.B. Hyde, A.F. Norman, and P.B. Prangnell: 'The effect of cooling rate on the morphology of primary Al$_3$Sc intermetallic particles in Al-Sc alloys', *Acta Mater.*, 2001, **49** (8), 1327–1337.

17. A.F. Norman, K. Hyde, F. Costello, S. Thompson, S. Birley, and P.B. Prangnell: 'Examination of the effect of Sc on 2000 and 7000 series aluminium alloy castings: for improvements in fusion welding', *Mater. Sci. Eng. A*, 2003, **354** (1–2), 188–198.

18. P.A. Rometsch, H. Zhong, K.M. Nairn, T. Jarvis, and X. Wu: 'Characterization of a laser-fabricated hypereutectic Al-Sc alloy bar', *Scr. Mater.*, 2014, **87**, 13–16.

19. K. Schmidtke, F. Palm, A. Hawkins, and C. Emmelmann: 'Process and mechanical properties: Applicability of a scandium modified Al-alloy for laser additive manufacturing', *Phys. Procedia*, 2011, **12**, 369–374.

20. Frank Palm, Airbus Defence and Space Gmbh: 'Aluminium material having improved precipitation hardening', US Patent 20150027595, published 29 January 2015.

21. Awadh. B. Pandey, United Technologies Corporation: 'High strength L12 aluminium alloys', US Patent 8002912, published 23 August 2011.

22. C.T. Horovitz, K.A. Gschneidner, G.A. Melson, D.H. Youngblood, H.H. Schock: 'Scandium: Its occurrence, chemistry, physics, metallurgy, biology and technology', 1975, London, Academic Press.

23. T.B. Massalski, H. Okamoto, P.R. Subramanian and L. Kacprzak: 'Binary alloys phase diagrams', 2nd edn, Vol. 3, 2109; 1986, ASM International.

24. M.J. Bu, Y.B. Peng, M. Wang, Y. Du, H.H. Xu, D.D. Zhao, and C.S. Sha: 'Thermodynamic optimization of the Sc-X (X = La, Li, Ca, Cr) systems', *J. Phase Equil. Diff.*, 2012, **33** (1), 40–45.

25. B. Predel: 'Sc-V' in 'Group IV Physical Chemistry', Vol. 5, 'Phase equilibria, crystallographic and thermodynamic data of binary alloys', Subvol. J, 'Pu-Re – Zn-Zr', (ed. Landolt-Börnstein), 1-2; 1998.

26. K.A. Gschneidner and F.W. Calderwood: 'The Ce-Sc (Scandium-Cerium) system', *Bull. Alloys Phase Diagrams*, 1982, **3** (2), 189-190.

27. H. Okamoto: 'Pd-Sc (Palladium-Scandium)', *J. Phase Equil.*, 2002, **23** (6), 554.

28. N.A. Sabirzynov: 'Phase equilibria and properties of Sc, Sm, Er, Yb, and Lu with thallium', PhD thesis, Chemistry Institute Ural Branch of Russian Academy of Science, Sverdlovsk, USSR, 1988,13-14.

29. H. Okamoto and T.B. Massalski: 'Binary alloy phase diagrams requiring further studies', *J. Phase Equil.*, 1994, **15** (5), 500-521.

30. A. Bilić, J.D. Gale, M.A. Gibson, N. Wilson and K. McGregor: 'Prediction of novel alloy phases of Al with Sc or Ta', *Sci. Reports*, 2015, **5**, 9909.

31. P.W. Voorhees: 'Alloys: scandium overtakes zirconium', *Nature Mat.*, 2006, **5**, 435-436.

32. K. Gschneidner, A. Russell, A. Pecharsky, J. Morris, Z. Zhang, T. Lograsso, D. Hsu, C.H. Chester, Y. Ye, A. Slager, D. Kesse: 'A family of ductile intermetallic compounds', *Nature Mat.*, 2003, **2**, 587-591.

33. B.Y. Kotur: 'Scandium binary and ternary alloys systems and intermetallic compounds', *Croatica Chem. Acta*, 1998, **71**, 635-658.

34. J.C. Zhao: 'The diffusion-multiple approach to designing alloys', *Ann. Rev. of Mat. Res.*, 2005, **35.**

35. J.C. Zhao, X. Zheng and D.G. Cahill: 'High-throughput measurements of material properties', *JOM*, 2011, **63**, 40–44.

36. H. Eckert and R. Pöttgen: '[45]Sc solid state NMR spectroscopy – A complementary Tool to X-tray crystallography for structure determination of intermetallic compounds', *Z. anorg. allg. Chem.*, 2010, **636**, 2232–2243 and references herein contained.

37. B. Ya Kotur and E. Gratz: 'Scandium alloy systems and intermetallics', in 'Handbook of the Physics and Chemistry of Rare Earths', Vol. 27, 339-533; 1999, Elsevier.

38. X. Tao, Y. Ouyang, H. Liu, Y. Du, Y. He and Z. Jin: 'Phase stability of Magnesium-Rare Earth binary systems from first-principles calculations.', *J. Alloys Comp.*, 2011, **509** (24), 6899-6907.

39. Pisch, F. Hodaj, P. Chaudouët and C. Colinet: 'Standard enthalpies of formation of some Mn-Y and Mn-Sc intermetallic compounds', J. *Alloys Comp.*, 2001, **319** (1-2), 210-213.

40. F.R. de Boer, W.C.M. Mattens, R. Boom, A.R. Miedema and A.K. Niessen: Cohesion in metals', Vol. 1, 1988, North Holland, Elsevier.

41. A. Pish and R. Schmid-Fetzer: 'Experimental study and thermodynamic assessment of phase equilibria in the Mn-Sc System', *Int. J. Mat. Res.*, 1998, **89** (10), 700-703.

42. V.S. Sudavtsova, M.O. Shevchenko, V.V. Berezutskii and M.I. Ivanov: 'Thermodynamic Properties of Liquid Fe-Sc Alloys', *Powder Metall. Met. Ceram.,* 2013**, 52** (7-8), 456-464.

43. N. Selhaoui and O.J. Kleppa: 'Standard enthalpies of formation of scandium alloys Sc+Me (Me= Fe, Co, Ni, Ru, Rh, Rd, Ir, Pt) by high-temperature calorimetry', *J. Alloys Comp.*, 1993, **191** (1), 145-149.

44. L.V. Goncharuk and V.R. Sidorko: 'Thermodynamics of interaction of rare-earth metals with d-metals. The Scandium-Iron system', *Powder Metall. Met. Ceram.*, 2001, **40** (7-8), 354-361.

45. X.J. Liu, P. Yu, C.P. Wang and K. Ishida: 'Thermodynamic evaluation of the Co-Sc and Fe-Sc systems', *J. Alloys Comp.*, 2008, **466** (1-2), 169-175.

46. Z. Du, Z. Jiang and C. Li: 'Thermodynamic optimization of the Ru-Sc system', *J. Alloys Comp.*, 2007, **427** (1-2), 148-152.

47. L.V. Goncharuk, V.R. Sidorko, V.G. Khoruzhaya and T.Ya. Velikanova: 'Thermodynamic parameters of scandium-iridium compounds ‹IrSc$_3$› and ScIr$_2$', *Powder Metall. Met. Ceram.*, 2000, **39** (1-2), 55-58.

48. A.I. Kononov and E.G. Polyakov: 'High-temperature electrochemical synthesis and properties of intermetallic compounds in the Ni-Sc system. Part 2: Thermodynamic and mechanical properties', *J. Alloys Comp.*, 1996, **239**, 107-110.

49. S. Kardellass, C. Servant, N. Selhaoui, A. Iddaoudi, M. Ait Amar and L. Bouirden: 'Thermodynamic description of the Ni-Sc system', *CALPHAD*, 2013, **42** (0), 59-65.

50. A.R. Miedema: 'Cohesion in alloys – fundamentals of a semi-empirical model', *Physica B+C*, 1979, **100** (1), 1-28.

51. M.A. Turchanin: 'Phase equilibria and thermodynamics of binary copper systems with 3d-metals. I. The copper-scandium system', *Powder Metall. Met. Ceram.*, 2006, **45** (3-4), 143-152.

52. L.F. Yamshchiko, A.G. Smirnov, A.G. Shubin and S.P. Raspopin: 'Thermodynamic properties of intermetallic compounds in the system Sc-Cu.', Proc. Republican Conf. on 'Physicochemical Bases of Metal Alloy Production', Alma Ata, Kazakhstan, June 1990.

53. S. Watanabe and O.J. Kleppa: 'Thermochemistry of alloys of transition metals. Part IV. Alloys of copper with scandium, yttrium, lanthanum and lutetium', *Metall. Mat. Trans. B*, 1984, **15B** (2), 357-368.

54. L.F. Yamshchikov, A.B. Shubin, S.P. Raspopin and A.G. Smirnov: 'Thermodynamic properties of intermetallics in the system Sc-Cu." *Metally*, 1991, **3**: 204-206.

55. V. Sidorko and L.V. Goncharuk: 'Thermodynamics of rare-earth metal interaction with copper', *Powder Metall. Met. Ceram.*, 2006, **4** (3-4), 136-142.

56. X.J. Liu, S.L. Wang and C.P. Wang: 'Thermodynamic assessments of the Sc-M (M: Ag, B and Th) systems', *J. Alloys Comp.*, 2009, **469** (1-2), 186-192.

57. K. Fitzner, W.-G. Jung and O.J. Kleppa: 'Thermochemistry of binary alloys of transition metals: The Me-Sc, Me-Y, and Me-La (Me=Ag,Au) systems', *Metall. Trans. A*, 1991, **22A**: 1103-1111.

58. A. Tang, P. Zhou, D.D. Zhao, X.M. Yuan, Y. Tang, P.S. Wang, B. Hu, Y. Du and H.H. Xu: 'Thermodynamic modeling of the Sc-Zn system coupled with first-principles calculation', *J. Mining Metall., Section B: Metall.*, 2012, **48** (1), 123-130.

59. L. Topor and O.J. Kleppa: 'Enthalpies of formation of first-row transition-metal diborides by a new calorimetric method', *J. Chem. Thermodynamics*, 1985, **17**, 1003-1016.

60. S.V. Meschel and O.J. Kleppa: 'Thermochemistry of alloys of transition metals and lanthanide metals with some IIIB and IVB elements in the periodic table', *J. Alloys Comp.*, 2001, **321**, 183-200.

61. G. Cacciamani, P. Riani, G. Borzone, N. Parodi, A. Saccone, R, Ferro, A. Pisch and R. Schmid-Fetzer: 'Thermodynamic measurements and assessment of the Al-Sc system', *Intermetallics*, 1999, **7**, 101-108.

62. M.O. Shevchenko, V.G. Kudin, V.V. Berezutskii, M.I. Ivanov and V.S. Sudavtsova: 'Thermodynamic properties of Al-Sc Alloys', *Powder Metall. Met. Ceram.*, 2014, **53** (3-4), 243-249.

63. W.-G. Jung, O.J. Klepp and L. Topor: 'Standard molar enthalpies of formation of PdAl, PtAl, ScAl$_{1.78}$, YAl$_2$ and LaAl$_2$', *J. Alloys Comp.*, 1991, **176**, 309-318.

64. S.V. Meschel and O.J. Kleppa: 'The standard enthalpies of formation of some 3d transition metal alumides by high-temperature direct synthesis calorimetry', in 'Metallic Alloys: Experimental and Theoretical Perspectives', Vol. 256, 'Series E: Applied Sciences', 103-112; 1994, Kluwer, Dordrecht, NATO ASI Series.

65. Z.K. Jun, L.B. Liu, H.S. Liu, X.M. Huang and Z.P. Jin: 'Thermodynamic assessment of the Ga-Sc and Ga-Tb systems', *J. Alloys Comp.*, 2008, **463** (1-2), 511-515.

66. A.K. Niessen, F.R. de Boer, R. Boom, P. F. de Châtel, W.C.M. Mattens and A.R. Miedema: 'Model prediction for the enthalpy of formation of transition metal alloys II', *CALPHAD*, 1983, **7** (1), 51-70.

67. Y.M. Golutvin, E.G. Maslennikova and L.G. Titov: 'Heats of formation of silicides in the scandium-silicon system', *Izv. Akad. Nauk. SSSR, Met.*, 1984, **6**, 47.

68. A. Qin, D. Liu, C. Chen, S. Liu, Y. Du, M. Wang and P. Nash: 'Heat contents of Sc$_5$Si$_3$ and ScSi intermetallics and thermodynamic modelling of the Sc-Si system', *J. Thermal Analysis Cal.*, 2015, **119** (2): 1315-1321.

69. S.V. Meschel and O.J. Kleppa: 'Standard enthalpies of formation of some 3d transition metal gallides by high-temperature direct synthesis calorimetry', *J. Alloys Comp.*, 1999, **290**, 150-156.

70. G.M. Lukashenko G.M. and R.I. Polotskaya: 'Thermodynamic properties of scandium, lanthanum, neodymium and gadolinium silicides and germanides', *J. Alloys Comp.*, 1992, **179**, 299-305.

71. A.K. Niessen and F.R. de Boer: 'The enthalpy of formation of solid corides, carbides, nitrides, silicides and phosphides of transition and noble metals', *Izv. Akad. Nauk. SSSR, Neorg. Mater.*, 1981, **18**, 518.

72. L. Topor and O.J. Kleppa: 'Standard enthalpy of formation of Sc_5Si_3', *Metall. Mat. Trans. B*, 1989, **20B**: 879-882.

73. K. Cheng, B. Hu, Y. Du, H. Xu and Q. Gao: 'Thermodynamic modelling of the Ge-Sc system supported by key experiments and first-principle calculation', *CALPHAD*, 2012, **37**, 18-24.

74. V.A. Lebedev, V.I. Kober and L.F. Yamschikov: 'Thermo-chemistry of Alloys of Rare-Earth and Actinide Elements, Handbook', *Metallurgiya*, Chelyabinsk, 1989.

75. A. Iddaoudi, N. Selhaoui, M. Ait Amar, S. Kardellass, R. Karioui and L. Bouirden: 'Thermodynamic assessment of the Sc-Sn system', *CALPHAD*, 2013, **41**, 71-75.

76. O.V. Podarevskaya: 'Thermodynamical properties of scandium, titanium and niobium stannides', PhD thesis, Franzevich Instutute for Problems in Materials Science, Kiev, Ukraine, 1992, 1-21.

77. S.V. Meschel and O.J. Kleppa: 'Standard enthalpies of formation of some rare earth stannides by high temperature direct synthesis', *J. Alloys Comp.*, 1996, **238**, 180-186.

78. E.J. Huber Jr., G.C. Fitzgibbon, E.L. Head, C.E. Holley Jr.: 'The heat of formation of scandium oxide', *The Journal of Physical Chemistry*, 1963, **67** (8), 1731-1733.

79. O.I. Bodak, B.Y. Kotur, I.S. Gavrilenko, V.Y. Markiv and V.G. Ivanchenko: 'Scandium-iron system phase diagram', *Dopov. Akad. Nauk Ukr. SSR*, **A 4**, 1978, 365–370.

80. R.I. Andrusyak and B.Y. Kotur: 'Phase equilibria in the Sc-Mn-Ge and Sc-Fe-Ge systems at 870 K', *Russ. Metall.*, 1991, **1991** (4), 204-208.

81. H. Okamoto: 'Fe-Sc (Iron-Scandium)', *JPEDAV*, 2012, **33**, 80.

82. G.S. Braslavskaya and S.B. Maslenkov: 'Intermediate phases $ScNi_5$ and Sc_2Ni_7 and polymorphism in $ScNi_5$', *Izv. Ak. Nauk SSSR, Metally*, 1987, **1**, 112-118.

83. S.B. Maslenkov and G.S. Braslavskaya: 'Phase diagram of Ni-Sc (up to 36 at%)', *Izv. Ak. Nauk SSSR, Metally*, 1984, **1**, 203-206.

84. J.A. Goebel and S. Rosen: 'Phase equilibria in the Scandium-Nickel-Aluminium system at 1000 °C', *J. Less-Common Met.*, 1968, **16** (4), 441.

85. D. Seipler, B. Bremicker, U. Goebel, H. Happel, H.E. Hoenig and B. Perrin: 'Electronic structure of intermetallic compounds with CsCl structure', *J. of Phys. F: Met. Phys.*, 1977, **7**, 599-611.

86. K.E. Kornienko and V.G. Khoruzhaya: 'Metal chemistry of scandium in binary systems formed with platinum-group metals as the basis for construction multicomponent systems based on those metals', *Powder Metall. Met. Ceram.*, 2001, **40**, 362-373.

87. X. Liu, R. Ehrl and K.-J. Range, 'High Pressure Synthesis and Structures of Scandium-Zinc Intermetallic Compounds $ScZn_2$, Sc_3Zn_{17} and $Sc_{13}Zn_{58}$', *Rev. High Pressure Sci. Technol.*, 1998, **7**, 1016-1018.

88. H.F. Braun and C.U. Segre: 'The superconductivity of $Sc_5T_4Si_{10}$ (T=Co, Rh, Ir) and isomorphous compounds', *Solid State Comm.*, 1980, **35**, 735-738.

89. D.C. Jhonston and H.F. Brown: 'Systematics of superconductivity in ternary compounds', in 'Superconductivity in ternary compounds II: Superconductivity and magnetism', Topics in Current Physics (ed. M.B. Maple and O. Fischer), 33-36; 1982, Springer-Verlag Berlin Heidelberg GmbH.

90. B.Y. Kotur: 'Crystal chemistry of ternary intermetallic compounds of scandium with transition metals and carbon, silicon or germanium', *J. Alloys Comp.*, 1995, **219**, 88-92.

91. M.Y. Teslyuk and W.M. Protasov: 'Crystal structures of ternary phases in the Al-Cu-Sc system', *Crystallography Rep*., 1965, **10** (4), 561-562.

92. M.L. Kharakterova: 'Phase composition of Al-Cu-Sc alloys at temperatures of 450°C and 500°C', *Russ. Metall.*, 1991, **4**, 195-199.

93. B.A. Chen, G. Liu, R.H. Wang, J.Y. Zhang, L. Jiang, J.J. Song and J. Sun: Effect of interfacial solute segregation on ductile fracture of Al-Cu-Sc alloys', *Acta Mater.*, 2013, **61**, 1676-1690.

94. M. Gazizov and R. Kaibyshev: 'Effect of over-aging on the microstructural evolution in an Al–Cu–Mg–Ag alloy during ECAP at 300 °C', *J. Alloys Comp.*, 2012, **527**, 163–175.

95. M. Jia, Z. Zheng and Z. Gong: 'Microstructure evolution of the 1469 Al-Cu-Li-Sc alloy during homogenization', *J. Alloys Comp.*, 2014, **614**, 131-139.

96. M. Gazizov, V. Teleshov, V. Zakharov and R. Kaibyshev: 'Solidification behaviour and the effects of homogenisation on the structure of an Al–Cu–Mg–Ag–Sc alloy', *J. Alloys Comp.*, 2011, **509**, 9497–9507.

97. H. Bo, L.B. Liu and Z.P. Jin: 'Thermodynamic analysis of Al-Sc, Cu-Sc Al-Cu-Sc system', *J. Alloys Comp.*, 2010, **490**, 318-325.

98. V. Raghavan: 'Al-Cu-Sc – Aluminium-Copper-Scandium', *J. Phase Equil. Diff.*, 2010, **31**, 554-555.

99. S. He, Y. Liu, Z. Li, H. Wu and B. Huang: 'Thermal stability and crystallization behaviour in Y-based metallic glasses', *Metall. Mat. Transactions A*, 2008, **39** (8), 1797-1803.

100. M.L. Kharakterova, N.G. Bukhanko, E.F. Kazakova and E.M. Sokolovskaya: *Russ. Metall.*, 2001, **4**, 425–431.

101. V. Raghavan: 'Al-Co-Sc (Aluminium-cobalt-scandium)', *J. Phase Equilibria Diff.*, 2009, **30** (2), 179-180.

102. P. Villars, K. Cenzual, R. Gladyshevkii: 'Handbook of inorganic substances 2015'; 2014, De Gruyter.

103.   P. Nandi, S. Suwas, S. Kumar, K. Chattopadhyay: 'The effect of minor additions of Ni on the microstructural evolution and mechanical properties of suction cast Al-0.14 at.pct Sc binary alloy', *Metall. Mat. Trans. A*, 2013, **44** (6), 2591-2603.

104.   D. Chen, C. Xia, Z. Chen,Y. Wu, M. Wang, N. Ma and H. Wang: 'Thermodynamic, elastic and electronic properties of $AlSc_2Si_2$', 2015, *Mat. Letters*, **138**, 148-150.

105.   L.L. Rokhlin, N.R. Bochvar, O.V. Rybal'chenko, I.E. Tarytina and A.V. Sukhanov: 'Phase equilibria in alumina-rich Al-Sc-Si alloy during solidification', *Russian Metall.,* 2012, **7**, 606-611.

106.   A.T. Tyvanchuk, T.I. Yanson, B.Ya Kotur, O.S. Zarechnyuk and M.L. Kharakterova: 'Isothermal section of the Sc-Al-Si system at 770 K', *Izv. Ak. Nauk SSSR, Metally*, 1988, 187-188.

107.   L.S. Toropova, T.V. Dobatkina and M.L. Kharakterova: 'Equilibrium in aluminum alloys of the Al – Si – Sc system', *Phys. Metall. Light Alloys*, 1985, 54-58.

108.   I.N. Fridlyander and L.V. Molchanova: 'Interaction of beryllium with aluminum and scandium', *Russ. Metall.*, 2003, **5**, 476-480.

109.   V. Raghavan: 'Al-Be-Sc (Aluminum-Beryllium-Scandium)', *J. Phase Equil. Diff.*, 2009, **30** (2).

110.   O.L. Semenova, N.Yu. Rusets'ka, T. Ya. Velikanova, and V.M. Vereshchak: 'Reactions in the crystallization of alloys in the Ti − Ni − Sc system in the TiNi − Ni − ScNi region', *Poroshk. Metall.*, 1996, **7-8**, 134-140.

111.   O.L. Semenova, N.Yu. Rusetskaya, and V.M. Petyukh: 'Projection of the solidus surface for the Sc − Ti − Ni system in the region of TiNi − Ni − ScNi alloys', *Poroshk. Metall.*, 1996, **11-12** (37-44).

112.   T.Ya. Velikanova, N. Yu. Krendelsberger, and O.L. Semenova: 'Phase equilibria in the melting-crystallization region for alloys in the Ti-TiNi-Sc0.53Ni0.47-Sc subsystem', *Powder Metall. Met. Ceram.*, 2005, **44** (9-10), 455-462.

113.   K.E. Kornienko, V.G. Khoruzha, and P.S. Martsenyuk: 'Alloy structure and equilibrium phase diagram for the Sc-Ru-Rh system. VII. Polythermal sections in the

Sc-Ru-Rh system', *Powder Metall. Met. Ceram.*, 2003, **42** (3-4), 165-170 and references herein cited.

114.   O.L. Semenova, Yu.V. Kudryavtsev, V.M. Petyukh and O.S. Fomichov: 'Constitution of Rh-Sc-Ti alloys in the 50% (at.) Rh section and adjacent composition range', *Powder Metall. Met. Ceram.*, 2013, **52** (7-8), 444-455.

115.   Y.V. Kudryavtsev and E.L. Semenova: 'High temperature thermomechanical properties of titanium-rhodium-based alloys containing scandium. Unusual shape memory effects observed in scandium-substituted alloy systems', *Platinum Met. Rev.*, 2014, **58** (1), 20–30.

116.   H. Holleck: 'Carbon and boron stabilized ordered phases of scandium', *J. Less-Common Met.*, 1977, **52**, 167.

117.   T.M. Gesing, K.H. Wachtmann, W. Jeitschko and Z. Naturforsch:' The perovskite carbides A(3)MC (A=Sc, Y, La-Nd, Sm, Gd-Lu; M=Al, Ga, In, Tl, Sn, Pb)', *Sect. B, J. Chem. Sci.*, 1997, **52** (2), 176.

118.   V.H. Nowotny: 'Strukturchemie einiger Verbindungen der Übergangsmetalle mit den elementen C, Si, Ge, Sn', *Prog. Solid State Chem.*, 1970, 2, 27.

119.   M. He, C.H. Wong, D. Shi, P.L. Tse, E-W. Scheidt, G. Eickerling, W. Scherer, P. Sheng and R. Lortz: '1D to 3D dimensional crossover in the superconducting transition of the quasi-one-dimensional carbide superconductor Sc_3CoC_4', *J. Phys.: Condens. Matter,* 2015, **27**.

120.   W. Scherer, C. Hauf, M. Presnitz, E.-W. Scheidt, G. Eickerling, V. Eyert, R-D. Hoffmann, Ute C. Rodewald, A. Hammerschmidt, C. Vogt and R. Pöttgen: 'Superconductivity in quasi one-dimensional carbides.', *Angew. Chem. Int. Ed.*, 2010, **49**, 1578–1582.

121.   Y. Shi, A. Leithe-Jasper and T. Tanaka: 'New Ternary Compounds $Sc_3B_{0.75}C_3$, $Sc_2B_{1.1}C_{3.2}$, $ScB_{15}C_{1.60}$ and Subsolidus Phase Relations in the Sc–B–C System at 1700 °C', *J. Solid State Chem.*, 1999, **148** (2), 250.

122.   Y.V. Milman, D.V. Lotsko and O.I. Sirko: ''Sc effect' of improving mechanical properties in aluminium alloys', 2000, *Mat. Sci. Forum*, **331-333** (1-3), 1107-1111.

123.   Y.V. Milman: 'Scandium effect on increasing mechanical properties of aluminium alloys', 2006, *High-temp. Mat. Proc.*, **25**, 1-10.

124.   E. Clouet, L. Laé, T. Épicier, W. Lefebvre, M. Nastar and A. Deschamps: 'Complex precipitation pathways in multicomponent alloys', *Nature Mat.*, 2006, **5**, 482-488.

125.   J. Røyset and N. Ryum: 'Scandium in aluminium alloys', *International Materials Review*, 2005, **50** (1), 19-44.

126.   W. Prukkanon, N. Srisukhumbowornchai and C. Limmaneevichitr: 'Modification of hypoeutectic Al–Si alloys with scandium', 2009, *J. Alloys Comp.*, **477**, 454-460.

127.   M. Fatih Kilicaslan, W-R. Lee, T.-H. Lee, Y. Sohn and S.-J. Hong: 'Effect of Sc addition on the microstructure and mechanical properties of as-atomized and extruded Al–20 Si alloys', 2012, *Mat. Lett.*, **71**, 164-167.

128.   S.L. Pramod, A.K. Prasada Rao, B.S. Murty and S.R. Bakshi: 'Effect of Sc addition on the microstructure and wear properties of A356 alloy and A356–TiB2 in situ composite', *Mat. Design*, 2015, **78**, 85-94.

129.   M. Kim: 'Electron back scattering diffraction (EBSD) analysis of hypereutectic Al-Si alloys modified by Sr and Sc', *Met. Mat. Int.*, 2013, **13**, 103-107.

130.   W. Prukkanon, N. Srisukhumbowornchai and C. Limmaneevichitr: 'Influence of Sc modification on the fluidity of an A356 aluminum alloy', *J. Alloys Comp.*, 2009, **487**, 453-457.

131.   U. Patakham, J. Kajornchaiyakul and C. Limmaneevichitr: 'Grain refinement mechanism in an Al–Si–Mg alloy with scandium', *J. Alloys Comp.*, 2012, **542**, 177-186.

132.   W. Zhang, Y. Liu, J. Yang, J. Dang, H. Xu and Z. Du: 'Effects of Sc content on the microstructure of As-Cast Al-7 wt.% Si alloys', *Mat. Characterization*, 2012, **66**, 104-110.

133.   V. Rajinikanth, K. Venkateswarlu, M. Kuntal Sen, M. Das, S.N. Alhajeric and T.G. Langdo: 'Influence of scandium on an Al–2% Si alloy processed by high-pressure torsion', *Mat. Sci. Eng. A*, 2011, **528**, 1702-1706.

134.   M. Kim, Y. Hong and H. Cho: 'The Effects of Sc on the Microstructure and Mechanical Properties of Hypo-Eutectic Al-Si Alloys', *Met. Mat. Int.*, 2004, **10**, 513-520.

135.   V.G. Davydov, T.G. Rostova, V.V. Zakharov, Y.A. Filatov and V.I. Yelagin: 'Scientific principles of making an alloying addition of scandium to aluminium alloys', *Mater. Sci. Eng. A*, 2000, **280**, 30–36.

136.   E. A. Marquis and D. N. Seidman: 'Nanoscale structural evolution of Al$_3$Sc precipitates in Al(Sc) alloys', *Acta Mater.*, 2001, **49**, 1909–1919.

137.   D. N. Seidman, E. A. Marquis and D. C. Dunand: 'Precipitation strengthening at ambient and elevated temperatures of heat-treatable Al(Sc) alloys', *Acta Mater.*, 2002, **50**, 4021–4035.

138.   E. A. Marquis, D. N. Seidman and D. C. Dunand: 'Erratum: Precipitation strengthening at ambient and elevated temperatures of heat-treatable Al(Sc) alloys', *Acta Mater.*, 2003, **51**, 285–287.

139.   M.E. Dalan, D.C. Dunand and D.N. Seidman: 'Effects of Ti additions on the nanostructure and creep properties of precipitation-strengthened Al–Sc alloys', *Acta Mater.*, 2005, **53**, 4225-4235.

140.   Y. Ali, D. Qiu, B. Jiang, F. Pan and M.-X. Zhang: 'Current research progress in grain refinement of cast magnesium alloys: A review article', *J. Alloys Comp.*, 2015, **619**, 639–651.

141.   Y. Lu and Z. Wang: 'Effects of rare earths on the microstructure, properties and fracture behavior of Mg–Al alloys', *Mater. Sci. Eng. A*, 2000, **278**, 66-76.

142. C.J. Bettles, M.A. Gibson and S.M. Zhuc: 'Microstructure and mechanical behaviour of an elevated temperature Mg-rare earth based alloy', *Mater. Sci. Eng., A*, 2009, **505**, 6–12.

143. T.L. Chia, M.A. Easton, S.M. Zhu, M.A. Gibson, N. Birbilis and J.F. Nie: 'The effect of alloy composition on the microstructure and tensile properties of binary Mg-rare earth alloys', *Intermetallics*, 2009, **17**, 481–490.

144. W. Tao, Z. Milin, N. Zhongyi and L. Bin: 'Influence of Rare Earth Elements on Microstructure and Mechanical Properties of Mg-Li Alloys', *J. Rare Earths*, 2006, **24**, 797 – 800.

145. S.B. Yin, B.Y. Huang and Z.M. Yin: 'Effect of minor Sc on high temperature mechanical properties of Ti–Al based alloys', *Mater. Sci. Eng. A*, 2000, **280**, 204–207.

146. H.Q. Liu, D.Q. Yi and F. Zheng: 'The influence of Sc on α/β transformation of Ti.', *Mater. Sci. Eng., A*, 2008, **487**, 58–63.

147. I.S. Jung, H.S. Jang, M.H. Oh, J.H. Lee and D.M. Wee: 'Microstructure control of TiAl alloys containing β stabilizers by directional solidification', *Mater. Sci. Eng. A*, 2002, **329–331**, 13-18.

148. D.M. Cupid: 'Thermodynamic Assessment Of The Ti-Al-Nb, Ti-Al-Cr, And Ti-Al-Mo Systems', PhD dissertation, University of Florida, Florida, USA, 2009, 48-111.

149. C.T. Yang and C.H. Koo: 'Improving the microstructure and high temperature properties of the Ti–40Al–16Nb alloy by the addition of a minor Sc or La-rich Misch metal', *Intermetallics*, 2004, **12**, 235–251.

150. J. Liu, Q.D. Luan, X.G. Wang and L.M. Peng: 'Microstructural and high temperature deformation characterization of Ti–45Al–3Nb–(Cr, Mn, Mo, Sc) alloy', *Mater. Sci. Eng. A,* 2010, **527**, 7658–7662

151. Q.D. Luan, Q.Q. Duan, X.G. Wang, J. Liu and L.M. Peng: 'Tensile properties and high temperature creep behavior of microalloyed Ti–Ti3Al–Nb alloys by directional solidification', *Mater. Sci. Eng. A*, 2010, **527**, 4484-4496.

152.   H.Q. Liu, D.Q. Yi, W.Q. Wang, L.P. Wang and C.B. Lian: 'Influence of Sc on high temperature strengthening behavior of Ti-6A1-4V alloy', *Trans. Nonferrous Met. Soc. China*, 2007, **17**, 1212-1219.

153.   Y.A. Filatov, V.I. Yelagin and V.V. Zakharov: 'New Al–Mg–Sc alloys', *Mater. Sci. Eng. A*, 2000, **280**, 97-101.

154.   K.L. Kendig and D.B. Miracle: 'Strengthening mechanisms of an Al-Mg-Sc-Zr alloy', *Acta Mater.*, 2002, **50**, 4165–4175.

155.   C.B. Fuller, A.R. Krause, D.C. Dunand and D.N. Seidman: 'Microstructure and mechanical properties of a 5754 aluminum alloy modified by Sc and Zr additions', *Mater. Sci. Eng. A*, 2002, **338**, 8–16.

156.   D.W. Suh, S.Y. Lee, K.H. Lee, S.K. Lim and K.H. Oh: 'Microstructural evolution of Al–Zn–Mg–Cu–(Sc) alloy during hot extrusion and heat treatments', *J. Mater. Process. Technol.*, 2004, **155–156**, 330–1336.

157.   T. Noda, M. Okabe, S. Isobe and M. Sayashi: 'Silicide precipitation strengthened TiAl', *Mater. Sci. Eng. A*, 1995, **192**, 774–779.

158.   H.S. Cho, S.W. Nam, J.H. Yun and D.M. Wee: 'Effect of 1 at.% nitrogen addition on the creep resistance of two phase TiAl alloy', *Mater. Sci. Eng. A*, 1999, **262**, 129–136.

159.   F. Appel, J.D.H. Paul, M. Oehirng, U. Frobel and U. Lorenz: 'Creep Behavior of TiAl Alloys with Enhanced High-Temperature Capability', *Metall. Mater. Trans. A*, 2003, **34**, 2149–2164.

160.   C-J Zhan and C-H Koo: 'Creep behavior of Ti–40Al–16Nb intermetallic alloy and strengthening effects of minor Sc', *Mat. Trans.*, 2006, **47** (2), 440-445.

161.   F. von Buch, J. Lietzau, B.L. Mordike, A. Pisch and R. Schmid-Fetzer: 'Development of Mg–Sc–Mn alloys', *Mater. Sci. Eng. A*, 1999, **263**, 1–7.

162.   B.L. Mordike: 'Development of highly creep resistant magnesium alloys.', *J. Mater. Proc. Technol.*, 2001, **117,** 391-394.

163.   I. Stulikova, B. Smola, F.V. Buch and B.L. Mordike: 'Mechanical properties and creep of Mg-rare earth-Sc-Mn squeeze cast alloys', *Materialwissenschaft und Werkstofftechnik*, 2003, **34**, 102-108.

164.   B. Smola, I. Stulikova, J. Pelcova and B.L. Mordike: 'Significance of stable and metastable phases in high temperature creep resistant magnesium-rare earth base alloys', *J. Alloys Comp.*, 2004, **378**, 196-201.

165.   B.L. Mordike, I. Stulikova and B. Smola: 'Mechanisms of creep deformation in Mg-Sc-based alloys', *Metall. Mater. Trans. A*, 2005, **36,** 1729-1736.

166.   M. Yang and F. Pan: 'Comparative studies on as-cast microstructures and mechanical properties between Mg-3Ce-1.2Mn-0.9Sc and Mg-3Ce-1.2Mn-1Zn magnesium alloys', *Trans. Nonferrous Met. Soc. China*, 2012, **22**, 53-59.

167.   O. Roder, T. Wirtz, A. Gysler and G. G.Lutjering: 'Fatigue of Al-Mg alloys with and without scandium', *Mater. Sci. Eng. A*, 1997, **234-236**, 181-184.

168.   T. Wirtz, G.Lutjering, A.Gysler, B.Lenczowski and R.Rauh: 'Fatigue properties of the aluminium alloys 6013 and Al-Mg-Sc', *Mat. Sci. Forum*, 2000, **331-337**, 1489-1494.

169.   A. Vinogradov, A. Washikita, K. Kitagawa and V.I. Kopylov: 'Fatigue life of fine-grain Al-Mg-Sc alloys produced by equal-channel angular pressing', *Mater. Sci. Eng. A*, 2003, **349**, 318–326.

170.   N. Stanford, G. Sha, J. Xia, S. Ringer and M. R. Barnett: 'Solute segregation and texture modification in an extruded magnesium alloy containing gadolinium', *Scr. Mater.*, 2011, **65** (10), 919–921.

171.   J. Hadorn, K. Hantzsche, S. Yi, J. Bohlen, D. Letzig, J. A. Wollmershauser and S. R. Agnew: 'Role of Solute in the Texture Modification During Hot Deformation of Mg-Rare Earth Alloys', *Metall. Mater. Trans. A*, 2012, **43A** (4), 1347–1362.

172.   F. Yang, F. Lv, X.M. Yang, S.X. Li, Z.F. Zhang, Q.D. Wang: 'Enhanced very high cycle fatigue performance of extruded Mg-12Gd-3Y-0.5Zr magnesium alloy'. *Mater. Sci. Eng. A*, 2011, **528**, 2231–2238.

173.   F.A. Mirza and D.L. Chen: 'Fatigue of rare-earth containing magnesium alloys: a review', *Fatigue Fract. Eng. Mater. Struct.*, 2014, **37**, 831–853.

174.   D. Griffiths: 'Review: Explaining texture weakening and improved formability in magnesium rare earth alloys', *Mat. Sci. and Tech.*, 2015, **31** (1), 10-24.

175.   K. Hantzsche, J. Bohlen, J. Wendt, K. Kainer, S. Yi and D. Letzig: 'Effect of rare earth additions on microstructure and texture development of magnesium alloy sheets', *Scr. Mater.*, 2010, **63** (7), 725–730.

176.   I.N. Igoshin, Y.A. Bazin, B.A. Baum, G.A. Raspopova and B.P. Domashnikov: 'Effect of scandium on properties of 35KHGSL steel in liquid and solid-state', *Steel in the USSR*, 1988, **18** (1), 39-40.

177.   T.V. Svistunova, O.S. Bobkova and B.D. Belyshov: 'Effect of scandium on structure and properties of corrosion-resistant steels', *Met. Sci. Heat Treat.*, 2008, 50 (5-6), 214-219.

178.   A.N. Sleptsov: 'The peculiarities of atomic ordering in scandium-doped austenitic FeCrNi alloys', Radiation Eff. Defects in Solids, 2000, 152 (3), 213-223.

179.   S.B. Maslenkov, G.S. Braslavskaya: 'Phase diagram of Ni-Sc (up to 36 at%)', *Izv. Ak. Nauk SSSR, Metally,* 1984, **1**, 203-206.

180.   D. Senk, F.M. Meyer, T. Pretz and G. Abrasheva: 'Strategies for fulfilment of critical raw materials demand in Europe', *Revue de Métallurgie*, 2012, 109, 333-339.

181.   A.S. Fedorov, G.N. Churilov, A.A. Kuzubov, M.V. Seriantova: 'Ab-initio investigation of hydrogen absorption by magnesium nanoparticles', in 'Carbon nanomaterials in clean energy hydrogen systems', NATO Science for Peace and Security, Series C, 'Environmental Security', 603-610; 2008, Springer.

182.   R.A.H. Niessen and P. H.L. Notten: 'Electrochemical Hydrogen Storage Characteristics of Thin Film MgX (X = Sc , Ti , V , Cr) Compounds', *Electrochem. and Solid-State Lett.*, 2005, **8**, A534-A538.

183.   W. P. Kalisvaart, R. A. H. Niessen, and P. H. L. Notten: 'Electrochemical hydrogen storage in MgSc alloys: A comparative study between thin films and bulk materials.', *J. Alloys Comp.*, 2006, **417** (1–2), 280–291.

184.   R. A. H. Niessen, P. H. L. Notten: 'Hydrogen storage in thin film magnesium-scandium alloys', *J. Alloys Comp.*, 2005, **404–406**(0):457–460.

185.   T. G. Manivasagam, K. Kiraz, P. H. L. Notten: 'Electrochemical and Optical Properties of Magnesium-Alloy Hydrides Reviewed', *Crystals*, 2012, **2**, 1410-1433.

186.   H.S. Brar, I.S. Berglund, J.B. Allen and M.V. Manuel: 'The role of surface oxidation on the degradation behaviour of biodegradable Mg–RE (Gd, Y, Sc) alloys for resorbable implants', *Mat. Sci. Eng. A*, 2014, **40**, 407–417.

187.   H.S. Brar, J.P. Ball, I.S. Berglund, J.B. Allen and M.V. Manuel: 'A study of a biodegradable Mg–3Sc–3Y alloy and the effect of self-passivation on the in vitro degradation', *Acta Biomater.*, 2013, **9**, 5331–5340.

188.   B.S. Murty, J.-W. Yeh and S. Ranganathan: 'High-Entropy Alloys', 1st ed; 2014, Elsevier.

189.   T. Zingg, T. Richmond and H.J. Guntherodt: 'Electronic transport properties of glassy Fe–Sc alloys', *Mater. Sci. Eng.*, 1988, **99**, 179.

190.   M.F. Braun, K.P. Scheltz, E.F. Wassermann and M. Ghafari: 'Relaxation studies of the remnant magnetization in the spin glass like state of amorphous $Fe_{90}(Zr_xSc_y)_{10}$ alloys', *J. Phys. Coll.*, 1988, **49** (C-8), 1165.

191.   D.R. Vujic, D.A. Lohemeier, and S.H. Whang: 'Occurrence of glassy phases in Sc-Co and Sc-Ni systems', *Int. J. Rapid Solid.*, 1990, **5**, 277.

192.   X.L. Wang, F. Jiang, H. Hahn, J. Li, H. Gleiter, J. Sun and J.X. Fang: 'Plasticity of a scandium-based nanoglass', *Scripta Mater.*, 2015, **98**, 40–43.

193.   X.K. Xi, S. Li, R.J. Wang, D.Q. Zhao, M.X. Pan, and W.H. Wang: 'Bulk scandium-based metallic glasses', *J. Mater. Res.*, 2005, **20** (9), 2243-2247.

194.   K.M. Youssef, A.J. Zaddach, C. Niu, D.L. Irving and C.C. Koch: 'A Novel Low-Density, High-Hardness, High-entropy Alloy with Close-packed Single-phase Nanocrystalline Structures', *Mater. Res. Lett.*, 2015, **3** (2), 95–99.

195.   S. Riva, C.M. Fung, J.R. Searle, R.N. Clark, N.P. Lavery, S.G.R. Brown, K.V. Yusenko: 'Formation and disruption of W-phase in High-Entropy Alloys' – *submitted*.

196.   S. Curtarolo, G.L.W. Hart, M. Buongiorno Nardelli, N. Mingo, S. Sanyito and O. Levy: 'The high-throughput highway to computational materials design', *Nature Mat.*, 2013, **12**, 191-201.